
GAZİ ÜNİVERSİTESİ
Gazi
1926

MICROSTRIP BAND-PASS FILTER DESIGN FOR 5G APPLICATION

Burak AÇIKALIN

IN PARTIAL FULFILLMENT OF THE REQUIREMENTS FOR THE DEGREE OF MASTER OF SCIENCE IN ELECTRICAL ELECTRONIC ENGINEERING DEPARTMENT

GAZI UNIVERSITY
GRADUATE SCHOOL OF NATURAL APPLIED SCIENCES

JANUARY 2025

ETHICAL STATEMENT

I at this moment declare that in this thesis study, I prepared the thesis writing rules of Gazi University Graduate School of Natural and Applied Sciences;

- All data, information, and documents presented in this thesis have been obtained within the scope of academic rules and ethical conduct,
- All information, documents, assessments, and results have been presented by scientific ethical conduct and moral rules,
- All material used in this thesis that is not original to this work has been exhaustively cited and referenced,
- No change has been made in the data used,
- The work presented in this thesis is original,

or else, I admit all loss of rights to be incurred against me.

Burak AÇIKALIN

30/01/2025

MICROSTRIP BAND-PASS FILTER DESIGN FOR 5G APPLICATION

(M. Sc. Thesis)

Burak AÇIKALIN

GAZİ UNIVERSITY

GRADUATE SCHOOL OF NATURAL AND APPLIED SCIENCES

January 2025

ABSTRACT

Microstrip filters have an important place in many electronic structures. With the recent rapid technological developments, the need for filters has increased. Recent developments have paved the way for 5G technology and expanded its application areas. It has led to the emergence of new frequency bands. Filters are systems that are used to block unwanted signals and are divided into types such as low-pass, high-pass, band-pass and band-stop. Band-pass filters are used to allow signals within a certain frequency range to pass while suppressing signals outside this range. In this thesis, the design and analysis of the band-pass filter designed for 3.5 GHz operation for 5G applications were performed and the measurement results were obtained. A 4th order Butterworth type band-pass filter was designed for our filter operating at 3.5 GHz. It was observed that the S_{11} (Return Loss) value of the filter with a center frequency of 3.5 GHz was around -30 dB and the S_{21} (Insertion Loss) value was around -1 dB. FR-4 with a dielectric constant of $\varepsilon_r = 4.3$ was selected as the substrate material and has a bandwidth of 300 MHz. The Printed Circuit Board (PCB) distributed element structure was used in the designs. The production of the filter operating at a center frequency of 3.5 GHz was carried out and similar results were obtained to the simulation results.

Science Code : 93415
Keywords : 5G, defected ground structure, butterworth, filter
Page Number : 53
Supervisor : Prof. Dr. Nursel AKÇAM
Second Supervisor : Asst. Prof. Dr. Burak DÖKMETAŞ

5G UYGULAMALARI İÇİN BANT GEÇİREN MİKROŞERİT FİLTRE TASARIMI

(Yüksek Lisans Tezi)

Burak AÇIKALIN

GAZİ ÜNİVERSİTESİ

FEN BİLİMLERİ ENSTİTÜSÜ

Ocak 2025

ÖZET

Mikroşerit filtreler birçok elektronik yapıda önemli bir yer tutmaktadır. Son zamanlardaki hızlı teknolojik gelişmeler ile birlikte filtre ihtiyacı artmıştır. Son gelişmeler 5G teknolojisinin önünü oldukça açmış ve uygulama alanlarını genişletmiştir. Yeni frekans bantlarının ortaya çıkmasına sebep olmuştur. Filtreler, istenmeyen sinyalleri engellemek için kullanılan sistemlerdir ve alçak geçiren, yüksek geçiren, bant geçiren ve bant durduran gibi türlere ayrılır. Bant geçiren filtreler, belirli bir frekans aralığındaki sinyallerin geçmesine izin verirken, bu aralık dışındaki sinyalleri bastırmak amacıyla kullanılır. Bu tez çalışmasında, 5G uygulamaları için 3.5 GHz çalışması için tasarlanan bant geçiren filtrenin tasarımı ve analizi yapılarak ölçüm sonuçları elde edilmiştir. 3.5 GHz 'de çalışan filtremiz için 4. dereceden Butterworth tipi bant geçiren filtre paralel kuplaj yapısı temel alınarak tasarlanmıştır. Merkez frekansı 3.5 GHz olan filtrenin ölçüm sonuçlarının S11 (Return Loss - Geri Dönüş Kaybı) değerinin -30 dB ve S21 (Insertion Loss - Ekleme Kaybı) değerinin -1 dB civarlarında olduğu gözlemlenmiştir. Dielektrik sabiti $\varepsilon_r = 4.3$ olan FR-4 alttaş malzemesi tercih edilmiş ve 300 MHz bant genişliğine sahip olacak şekilde hesaplamaları yapılmıştır. Tasarımlarda baskı devre kartı (Printed Circuit Board - PCB) üzerinde dağılmış eleman yapısı kullanılmıştır. 3.5 GHz merkez frekansında çalışan filtrenin üretimi gerçekleştirilmiş ve simülasyon sonuçlarına benzer sonuçlar elde edilmiştir.

Bilim Kodu : 93415
Anahtar Kelimeler : 5G, Kusurlu zemin yapısı, butterworth, filtre
Sayfa Sayısı : 53
Danışman : Prof. Dr. Nursel AKÇAM
İkinci Danışman : Dr. Burak DÖKMETAŞ

ACKNOWLEDGEMENTS

I would like to thank my main advisor Prof. Dr. Nursel AKÇAM and my co-advisor Dr. Burak DÖKMETAŞ for their support during the planning and execution phase of this thesis. I owe a debt of gratitude to my mother Yurdagül AÇIKALIN and my father Metin AÇIKALIN, who were always with me in this work.

CONTENTS

Page

ABSTRACT iv

ÖZET v

ACKNOWLEDGEMENTS vi

CONTENTS vii

LIST OF TABLES ix

LIST OF FIGURES x

SYMBOLS AND ABBREVIATIONS xii

1. INTRODUCTION 1

2. MICROWAVE BASICS 5

2.1. Filters by Element Usage 5

2.1.1. Active filters 5

2.1.2. Passive filters 6

2.2. Filters by Functions 6

2.2.1. Bandpass filter 7

2.2.2. Stop band filter 8

2.2.3. Low pass filter 10

2.2.4. High pass filter 11

2.3. Microwave Network Structure 12

2.3.1. Network variables 12

2.3.2. Scattering matrix 13

2.3.3. Z and Y matrices 15

2.3.4. ABCD parameter 16

2.3.5. Transmission line network 17

Page

2.4. Microstrip Lines and Components 18

2.4.1. Effective dielectric constant and characteristic impedance 19

2.4.2. Directed wavelength propagation constant 20

2.5. Filter Design Methods 21

2.5.1. Image parameter method 21

2.5.2. Insertion loss method 22

2.6. Filter Transformations and Application 25

2.6.1. Frequency and impedance scaling 26

2.6.2. Richard's transformations 28

2.6.3. Kuroda identities 29

3. DESIGN AND MANUFACTURE OF BANDPASS FILTER 31

3.1. Parallel Coupling 3.5 GHz Bandpass Filter Design 32

3.1.1. Butterworth lowpass LC filter prototype 32

3.1.2. 4th degree low pass filter design and band-pass filter design 33

3.1.3. Dimensional calculations of bandpass microstrip filter 37

3.2. Production and Measurement of the Designed 3.5 GHz Bandpass Filter 43

4. CONCLUSIONS AND RECOMMENDATIONS 47

REFERECENS 48

CURRICULUM VITAE 53

LIST OF TABLES

Table **Page**

Table 2.1. Filter transformation 28

Table 2.2. Equality of the four curos..... 30

Table 3.1. Filter properties 32

Table 3.2. Butterworth low-pass filter values 33

Table 3.3. 4th order ınductor and capacitor values 35

Table 3.4. Parallel coupling bandpass filter values 37

Table 3.5. Calculated filter dimensional parameters 38

Table 3.6. Optimized dimensional values 40

Table 3.7. Comparison of similar studies..... 43

LIST OF FIGURES

Figure **Page**

Figure1.1. Development of the communication generation 1

Figure 2.1. Filter usage 5

Figure 2.2. Bandpass bulk element filter circuit 7

Figure 2.3. Bandpass filter graphic 8

Figure 2.4. Band stop filter circuit 9

Figure 2.5. Band stop filter Chart 9

Figure 2.6. Low pass filter circuit 10

Figure 2.7. Low pass filter graph 11

Figure 2.8. High pass filter circuit 11

Figure 2.9. High pass filter chart 12

Figure 2.10. Two-Door network structure 13

Figure 2.11. ABCD parameter notation 17

Figure 2.12. Microstrip transmission structure 18

Figure 2.13. Two-door ABCD matrix 21

Figure 2.14. General filter design process block 23

Figure 2.15. Maximum flatness filter graph 23

Figure 2.16. Chebyshev low-pass 3rd order filter response 24

Figure 2.17. Elliptical filter frequency response 25

Figure 2.18.Frequency and impedance for low-pass and high-pass filter Scaling 26

Figure 2.19. Bandpass and bandstop conversions 28

Figure 3.1. Butterworth normalized frequency attenuation chart 33

Figure 3.2. Prototype circuit passing lower than 4th degree 34

Figure 3.3. 4th Degree bandpass filter circuit with bulk elements 35

Figure **Page**

Figure 3.4. Bandpass filter admittance transducer 35

Figure 3.5 4th order bandpass filter ads dimensional calculations 39

Figure 3.6. Standard parallel coupling bandpass filter structure 40

Figure 3.7. Recommended bandpass filter structure 41

Figure 3.8. Bandpass filter return loss(s_{11}) and ınsertion loss results(s_{21}) 41

Figure 3.9. Bandwidth graph of the bandpass filter 42

Figure 3.10. Bandpass filter group latency graph 42

Figure 3.11. Bandpass filter surface current distribution 43

Figure 3.12. The front side of the manufactured filter 44

Figure 3.13. Back side of the produced filter 44

Figure 3.14. Measurement stage of the produced filter 45

Figure 3.15. S11 and S21 results of the produced filter 45

Figure 3.16. Q11 simulation and production result comparison 46

Figure 3.17. S21 simulation and production result comparison 46

SYMBOLS AND ABBREVIATIONS

The symbols and abbreviations used in this study are presented below with their explanations.

Symbols	**Explanations**
db	decibel
ghz	Gigahertz
hz	Hertz
mm	Millimeter
ohm	Ohm

Abbreviations	**Explanations**
DC	Direct Current
DGS	Defected Ground Structure
G	Generation
IL	Insertion Loss
L	Inductance Capacitance
PCB	Printed Circuit Board
RF	Radio Frequency
RL	Return Loss
TEM	Transverse ElectroMagnetic

1. INTRODUCTION

The history of wireless communication goes back a long way. However, modern wireless communication technology was introduced in the 19th century. It started the century with the discovery of electromagnetic waves. People have long worked on wireless communication in order to communicate in large areas and over long distances. Significant progress was made when Marconi, a pioneer in wireless communication, invented the telegraph [1]. In the following periods, communication technology has constantly advanced and renewed. After the introduction of the first 1G (1 Generation) system in cellular network structures, a new generation emerges every 10 years in the light of important developments. After a long period of time and research, 1G, 2G, 3G, 4G and most recently 5G communication structures play an important role in the development of societies and the increase of production capabilities (Figure 1.1) [2].

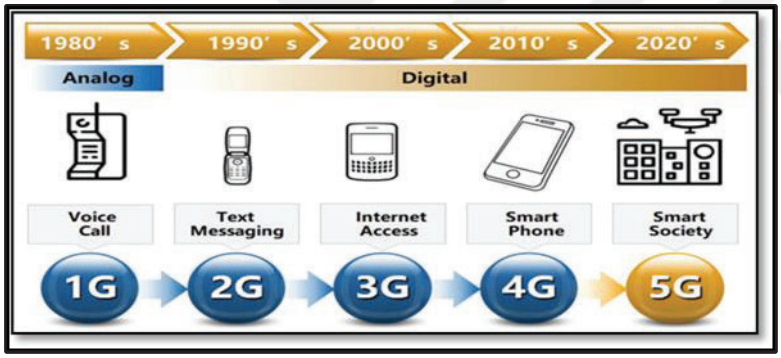


Figure 1.1. Development of the communication generation

5G has an important place in wireless communication. This system has many advantages over previous generations. One of its most important features is its ability to provide data transfer at high speeds. Theoretically, it shows download performance at gigabit speeds. This allows users to watch videos in high resolution, download and upload quickly, and play games and other internet-based applications more stable. Latency can be reduced to milliseconds, and this is an important parameter in live streaming, virtual reality, and real-time gaming. Another benefit is that it supports multiple connections. Smart devices, IoT-based offers simultaneous connection support for devices and devices such as many other devices.

In addition to these, high security, accessibility and low power consumption are among the benefits it provides [3]. Up to 4G, mobile communication technology uses frequency bands below 3 GHz, while in 5G, the frequency bands are FR-1 (410 MHz – 7125 MHz) and FR-2 (24.25 GHz – 52.5 GHz). Where user demand is high, high frequencies such as 26 – 28 GHz are preferred [4].

Microwave frequency refers to electromagnetic waves covering the range of 300 MHz – 300 GHz. Their wavelength is between 1m and 1mm [5]. Microwave filters are one of the important parts of communication systems. A filter is a communication element that provides two-door frequency control that transmits signals in a certain frequency range and stops unwanted signals in the other range [6].

The history of microwave filters goes back to the beginning of the 20th century. The widespread use of new technological devices in the Second World War increased the importance of microwave filters. After the war, developing technology gained momentum with new filter structures and optimization techniques, resulting in complex, high-performance filters. Microwave filters are used in wireless communication systems, radar systems, satellite communication, transceiver systems and many high frequency applications.

Microstrip filters are inexpensive, small-sized, economical, low-loss, compact design, microwave filters that provide high frequency performance and flexibility at desired frequencies with passive circuit elements such as capacitors and inductors [7-9]. These structures are low-profile, suitable for planar and non-planar surfaces, simple and inexpensive to manufacture using modern printed circuit technology. Adaptive elements with variable resonant frequency, impedance and pattern can be designed by adding pins and varactor diodes between the patch and the ground. Many commercial substrates are available for use in its design and manufacture [10].

Today, most computer-based design tools use the insertion loss method. Insertion loss is the loss of signal strength caused by the addition of a device to the transmission line and is expressed in decibels [11].

In the literature, there are versions of the bandpass filter that have been examined at different

degrees with different techniques. Since it is desired to have as little fluctuation as possible, the use of the Butterworth technique in the thesis was preferred [11]. Many methods such as parallel coupling, step impedance, interdigital, capacitive coupling have been used. In this thesis, a reduced size of the parallel coupling structure by bending it was used for the first design. It has been observed that the defected ground structure used in many band-pass designs in the literature provides great benefits in filter performance [12].

In this thesis, a bandpass filter was designed for 5G application. The speed and capacity increase provided by the use of filters determined the cut-off frequencies of 5G. First, a twisted parallel-coupled bandpass filter with a center frequency of 3.5 GHz and a bandwidth of 300 MHz was designed from the 4th order. In these filters, frequency suppression at -30 dB levels is obtained. It is thought that it will be useful for 5G applications due to its high selectivity and low insertion loss effect.

In the second part of the thesis, filter structures and techniques used are mentioned. Provides information about microwave network structures, parameters and analysis of filter systems. The methods used in the transformation of a low-pass filter into a band-pass filter structure are mentioned and how to make dimensional calculations according to the requirement characteristics in microstrip lines are explained.

In the third part of the thesis, the designs of bandpass filters were carried out according to their properties. First of all, after the transmission line calculations of the filters with LC circuits installed, their drawings were made in the CST program. The results of 5G filters with two different frequencies, 3.5 GHz and 28 GHz, were examined through the CST program.

2. MICROWAVE FILTER BASICS

Filters are an integral part of today's modern communication systems, and without understanding them, the full functioning of many communication systems cannot be understood. A filter is a network, usually a two-port, used in microwave systems to control the transmission or interception of a particular frequency band. These systems increase the transmission at a certain point in the frequency transition band and attenuate the signal in the stop band. In this way, they are used to achieve the desired frequency response in microwave systems [6] (Figure 2.1).

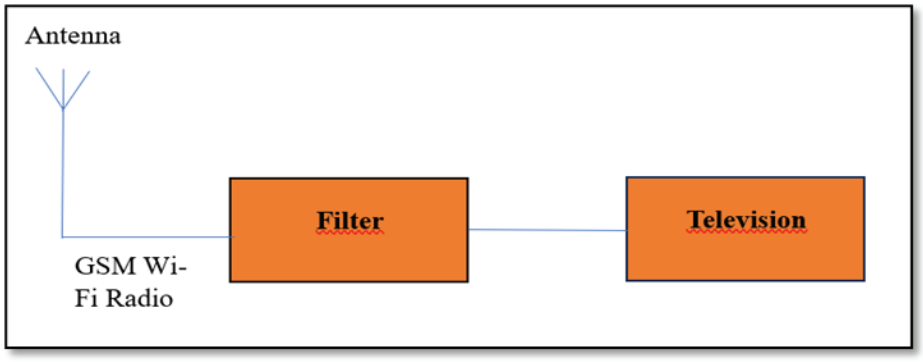


Figure 2.1. Filter usage

2.1. Filters by Element Usage

Filter structures are divided into active and passive filters according to their usage patterns.

2.1.1. Active filters

Active filters, which are frequently used in electrical circuits, are electronic devices that pass or stop a certain frequency range. These filters are designed to process signals of various frequencies, change their amplitude or pass the signal. They are used in many areas such as audio, video, Radio Frequency (RF), communication systems, and digital signal processing.

Active components, which usually consist of components such as transistors and operational amplifiers, improve the performance of the filter circuit and allow to control the filtering function more precisely.

There are many types of active filters, including low-pass, high-pass, band-pass, band-stop, and filters with a variety of specific frequency responses. For example, a low-pass filter intercepts high-frequency signals while passing low-frequency signals at a given cut-off frequency.

The advantages of active filters over passive filters are that they have higher gain, lower noise, better cutting characteristics. However, active filters also have some drawbacks, such as complexity and power consumption.

These filters have a wide range of applications, from audio systems to radio frequency receivers and from communication systems to medical devices. In particular, the requirements for digital signal processing and separation of frequency bands in modern communication systems further increase the importance of active filters [12].

2.1.2. Passive filters

Passive filters are one of the cornerstones of electrical circuits. These filters consist of passive components such as resistors, Capacitors (C) and Inductors (L) and are used to process signals of various frequencies. Their main purpose is to pass or intercept signals in a certain frequency range.

Passive filters are a circuit element that changes their behavior, usually depending on the signal frequency. For example, low-pass filters pass low-frequency signals, while high-frequency signals are intercepted. High-pass filters, on the other hand, do the opposite. The variety of these filters enables the design of customized filters for different application areas. Passive filters are generally simpler and lower cost, but active filters provide more flexibility and control.

2.2. Filters by Function

Filters are classified depending on the frequency of the signals. The type of filter is determined by the way the circuit elements are connected to the output signals. These filters allow signals to pass through unchanged in a certain frequency band range, while attenuating unwanted signals. The amplitude response of an ideal filter is described using the frequency

response curve of four different types of filters.

2.2.1. Bandpass filter

Bandpass filters are electronic circuits that pass signals in a specific frequency band and block frequencies outside that range. Theoretically, bandpass filters are defined by amplitude-frequency characteristics. This frequency curve indicates in which frequency range the filter will pass and which it will block.

Basically, the bandpass filter can be obtained by adding low-pass and high-pass filters end-to-end. It consists of parallel inductors and capacitors connected to the circuit shunted to the circuit attached to the inductors and capacitors connected in series to the circuit.

A bandpass filter is usually defined by three main parameters: center frequency (f_c), bandwidth (BW) and transition region. The center frequency indicates the frequency at which the filter transmits the most. Figure 2.2 shows the width of the pass through region between the BW, the undercut frequency (f_a) and the upper cut frequency (f_u). If the frequency of the lower cut is subtracted from the upper cut frequent, there is a range in the form of $BW=f_u-f_a$. The transition zone refers to the frequency range in which there is a transition between the transition band and the stop band of the filter [12]. The figure below shows the LC circuit structure.

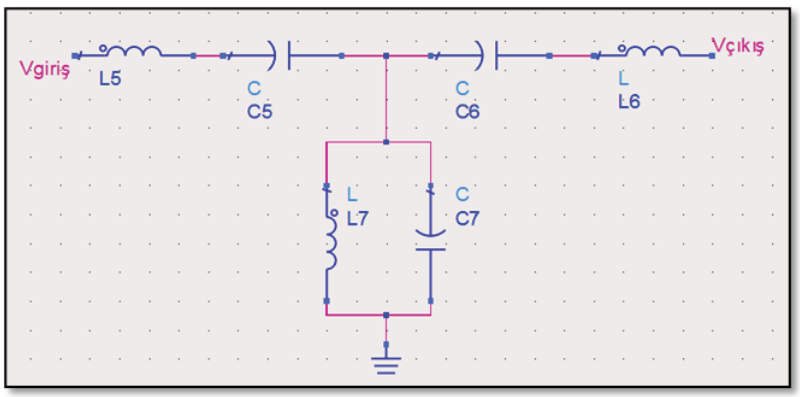


Figure 2.2. Bandpass bulk element filter circuit

Bandpass filters are used in many application areas. In wireless communication systems, for example, they are used to selectively pass signals in the frequency band of a particular

channel. It is one of the first places where the signal from the antenna is processed in transceiver systems.

However, bandpass filters also have some drawbacks. An ideal bandpass filter is difficult to achieve in practice. In real applications, the amplitude response of filters can be affected by factors such as phase loss and transition zone. Therefore, the design and application of filters should be done carefully and filter performance should be constantly monitored. Figure 2.3 below shows the amplitude-frequency graph of a bandpass filter.

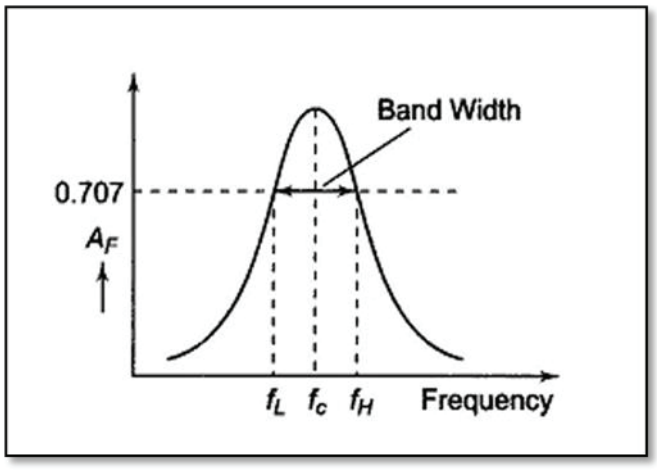


Figure 2.3. Bandpass filter chart

2.2.2. Stop band filter

Band stop filters are passive components within electronic circuits that block signals in a specific frequency band and pass other frequencies. These filters are often used to suppress unwanted signals or to filter signals in a certain frequency range. The key components of passive band-stopping filters are resistors, capacitors, and inductors (Figure 2.4). By combining these elements correctly, the damping process in a certain frequency band and the passage of signals at other frequencies are achieved [13].

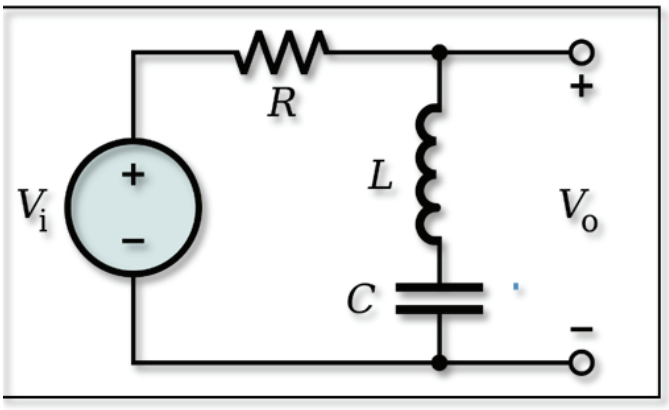


Figure 2.4. Band stop filter circuit

Band-stopping filters are especially commonly used in high-frequency applications such as RF communication systems, wireless communications, and radar systems. For example, in a wireless communication system, the use of band-stopping filters is preferred to suppress unwanted interference or interference signals.

Band-stopping filters are optimized to provide maximum damping in the desired frequency range (Figure 2.5). Throughout the design process, filter parameters are carefully selected and the characteristic features of the filter designed for a particular frequency band are obtained. The advantages of these filters include their simple structure, low cost, and effective signal filtering capabilities.

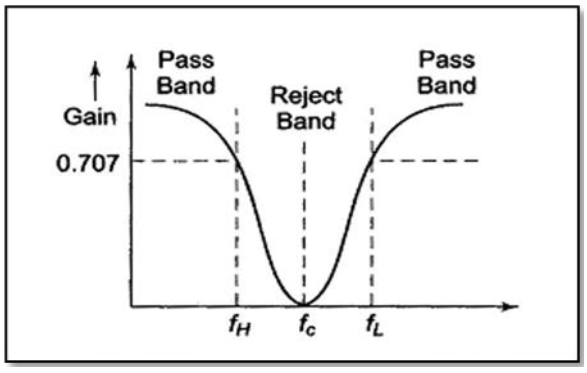


Figure 2.5. Band stop filter chart

Active band-stopping filters are electronic circuits that contain active components connected to the power supply, as opposed to passive band-stopping filters. They use active filters, operational amplifiers, and other active components.

2.2.3. Low pass filter

Low-pass filters play an important role in electronic signals. These are filtering circuits that block high frequencies while preserving low-frequency components. For example, they pass signals with a frequency lower than a certain cutoff frequency, while stopping those that are higher than the cutoff frequency. This is especially useful for blocking out unwanted high-frequency noise or interference in a given frequency band.

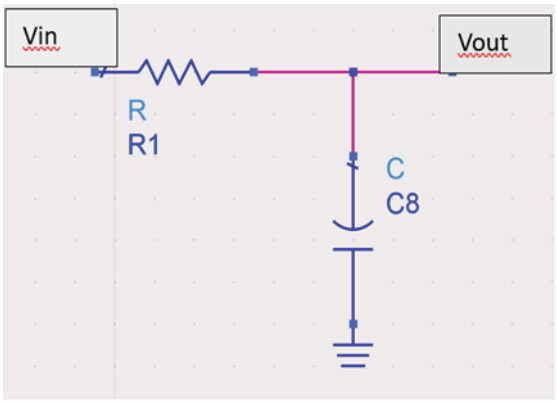


Figure 2.6. Low pass filter circuit

Low-pass filters have a variety of applications. It is preferred in electronic data transmission to improve the quality of signals and reduce transmission errors.

These filters usually require passive components such as resistors, capacitors and inductors (Figure 2.6). Passive low-pass filters can be connected to the signal processing circuit without the need for any power supply, while active low-pass filters use operational amplifiers or other active elements to create more complex circuits.

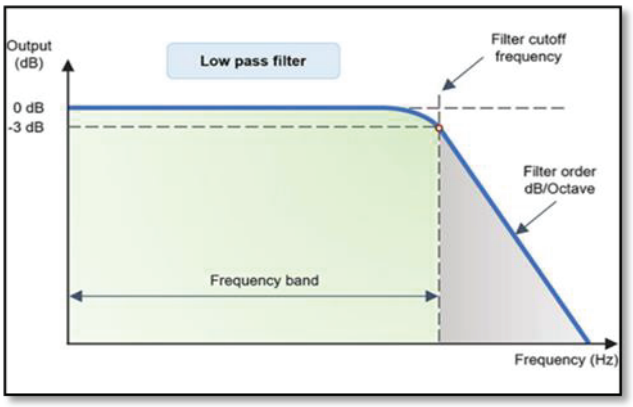


Figure 2.7. Low pass filter chart

The frequency response of low-pass filters indicates how the filter behaves (Figure 2.7). Parameters such as cut-off frequency, pass-band, and stop band determine the performance of the filter. The cut-off frequency is where the power is halved, that is, there is a drop of 3dB (decibel). It passes the signal below it and suppresses the part above it. As a result, low-pass filters occupy an important place in many areas by preserving low-frequency signals and blocking high-frequency unwanted signals in electronic systems [5].

2.2.4. High pass filter

High-pass filters are important elements used in electronic devices to suppress low-frequency noise or to isolate unwanted low-frequency signals. Figure 2.8 shows a schematic representation of a passive high-pass filter.

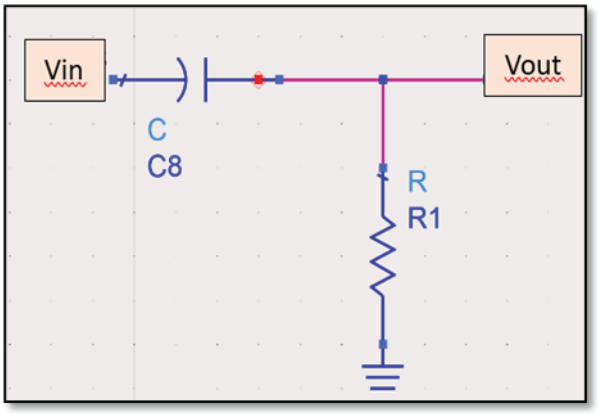


Figure 2.8. High pass filter circuit

Capacitors act as an open circuit at low frequencies and do not allow the passage of the

signal, but at high frequencies they act as a short circuit, allowing the passage of signals. In this circuit, a simple high-pass filter circuit with a capacitor and a resistor is shown (Figure 2.8). After the signal reaches the cut-off frequency (f_c) point, it starts to transmit (Figure 2.9). This point is actually the frequency point when it reaches the ground of -3 dB [14].

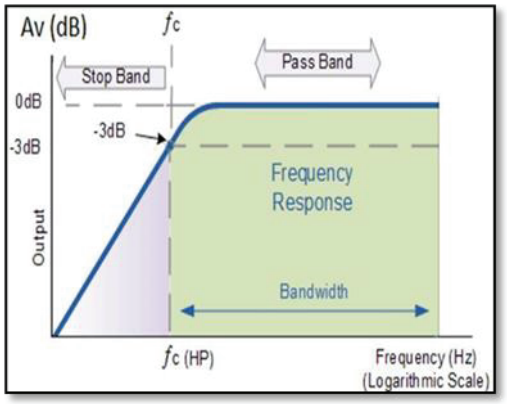


Figure 2.9. High pass filter chart

2.3. Microwave Network Structure

Although the realization of different frequencies varies in applications, the circuit network structure is the same for all of them. There is no direct use of conventional measuring devices for measuring current and voltage at microwave frequencies. In order to take advantage of low-frequency network calculations, the concepts of voltage, current, and impedance must be defined in terms of the network parameters of a filter [5].

2.3.1. Network variables

Most microwave filters and their components are expressed in 2-gate networks, as shown in Figure 2.10. Voltage and current values are complex variables.

$$\frac{V_1}{I1} = Z_{01} \tag{2.1}$$

$$\frac{V_2}{I2} = Z_{02} \tag{2.2}$$

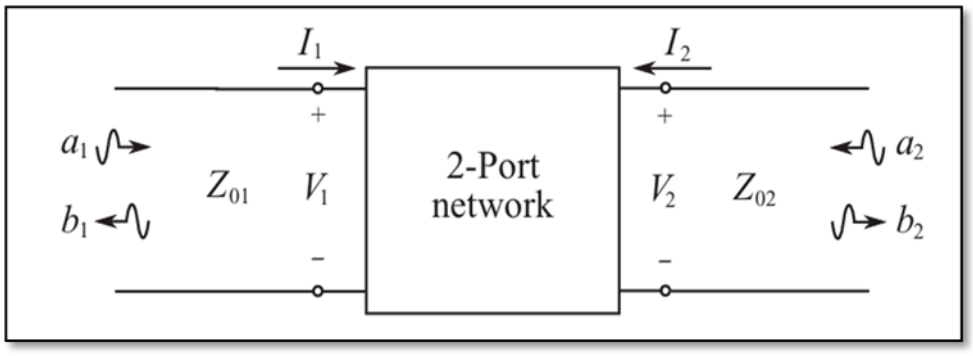


Figure 2.10. Two-Port network structure

2.3.2. Scattering matrix

The scattering parameter (S-parameters) is a measurement that describes the relationships of electrical signals in the RF and microwave circuit. This parameter is used in the design, analysis and optimization of circuits. The S-parameter determines the reflection and transmission of the signal applied to the terminal at the input terminal or the terminal at the output terminal at the other terminals. Measurements are usually made using RF measuring devices such as network analyzers and spectrum analyzers. S-parameters are generally valid within a certain frequency range. In two-gate circuits, a specific element of the scattering parameters is defined as in Eq.(2.1) [6].

$$S_{ij} = \frac{V_i^-}{V_J^+} |v_k^+ = 0 \text{ for k} \neq j \tag{2.3}$$

Where;

V_i^- = i'th terminal reflected wave voltage amplitude

V_J^+ = Wave voltage amplitude from the j'th terminal

In order to avoid reflections, the incoming waves at all terminals except the j'th terminal should be set to zero in the mapping with the loads.

$$b_1 = a_1 S_{11} + a_2 S_{12} \tag{2.4}$$

$$b_2 = a_1 S_{21} + a_2 S_{22} \tag{2.5}$$

The scattering matrix is expressed in the 2x2 form as in Eq.(2.4)

$$S = \begin{bmatrix} S_{11} & S_{12} \\ S_{21} & S_{22} \end{bmatrix} \tag{2.6}$$

Scattering parameters

$$S_{11} = \frac{b_1}{a_1} | a_2 = 0 \qquad S_{12} = \frac{b_1}{a_2} | a_1 = 0 \tag{2.7}$$

$$S_{21} = \frac{b_2}{a_1} \Big| a_2 = 0 \qquad S_{22} = \frac{b_2}{a_2} \Big| a_1 = 0 \tag{2.8}$$

S_{11} and S_{22} represent the reflection coefficients, and S_{12} and S_{21} represent the transmission coefficients. Thanks to the S parameters, current and voltage values can be measured with the transmitted wave and the reflected wave. S parameters are expressed in dB and are logarithmically represented as shown in Eq.(2.6).

$$20 \log |S_{mn}| \, dB \qquad m, n = 1,2 \tag{2.9}$$

The two parameters that determine the filter character are:

$$L_A = -20 \log |S_{mn}| \, dB \qquad \text{m, n=1,2 } (m \neq n) \tag{2.10}$$

$$L_R = 20 \log(|S_{mn}| \, dB \qquad \text{n=1, 2} \tag{2.11}$$

Where; n and m refer to the insertion loss between terminals.
As a result, the scattering matrices S_{11} and S_{22} are expressed as the characteristic impedance (Z_0) and the impedance at the input terminal (Z_{in1}) in terms of the impedance at the output terminal in Eq. (2.8).

$$\mathrm{Z_{in1}} = \frac{\mathrm{V_1}}{\mathrm{I_1}}, \tag{2.12}$$

$$\mathrm{S_{11}} = \frac{\mathrm{Z_{in1} - Z_{01}}}{\mathrm{Z_{in1} + Z_{01}}} \quad , \quad \mathrm{S_{11}} = \frac{\mathrm{Z_{in2} - Z_{02}}}{\mathrm{Z_{in2} + Z_{02}}} \tag{2.13}$$

S- parameters have many useful features in network analysis. The reflection coefficient is known as the transmission coefficient or voltage gain. The symmetric network also has the property of reciprocity. In a lossless passive network, the transmitted and reflected power

must be equal to the total incoming power. The mathematical explanation of this statement is as follows [15].

$S_{11} = S_{22}$ (If the network is symmetrical) (2.14)

$S_{12} = S_{21}$ (If the network is mutual) (2.15)

$S_{21}S_{21}^{*} + S_{11}S_{11}^{*} = 1$ or $|S_{21}|^2 + |S_{11}|^2 = 1$ (2.16)

$S_{21}S_{21}^{*} + S_{11}S_{11}^{*} = 1$ or $|S_{12}|^2 + |S_{22}|^2 = 1$ (2.17)

Frequency dependency examination is performed to determine the correct operating frequency range in RF and microwave circuits. It is used to describe certain properties such as stability, bandwidth, gain, reflection losses, and insertion losses of circuits. These parameters are useful in the evaluation of the design and analysis of circuits.

2.3.3. Z and Y matrices

The relationship between voltage and current at each terminal can be defined by the impedance network as given in below equations.

$V_1 = Z_{11}I_1 + Z_{12}I_2$ (2.18)

$V_2 = Z_{21}I_1 + Z_{22}I_2$ (2.19)

The impedance is known as a matrix or Z-matrix.

$$[Z] = \begin{bmatrix} Z_{11} & Z_{12} \\ Z_{21} & Z_{22} \end{bmatrix} \quad (2.20)$$

$Z_{11} = \frac{V_1}{I_1}\Big|_{I_2 = 0} \quad Z_{12} = \frac{V_1}{I_2}\Big|_{I_1 = 0}$

(2.21)

$Z_{21} = \frac{V_2}{I_1}\Big|_{I_2 = 0} \quad Z_{22} = \frac{V_2}{I_2}\Big|_{I_1 = 0}$ (2.22)

The 4 inputs of [Z] are known as open-loop impedances and are referred to as the [Z] open stream impedance matrix. Due to this feature, it is frequently used in serial network

connection. The inverse matrix [Y] is known as the short-circuit admittance matrix. Y-matrix

$$[\mathrm{Y}] = [Z]^{-1} = \begin{bmatrix} Y_{11} & Y_{12} \\ Y_{21} & Y_{22} \end{bmatrix} \tag{2.23}$$

In contrast to the open-circuit impedance parameter equation, the short-circuit admittance parameter is derived from the short-circuit definition at the n'th terminal.

$$\mathrm{Y}_{11} = \frac{\mathrm{I}_1}{\mathrm{V}_1} \Big| \mathrm{V}_2 = 0 \qquad \mathrm{Y}_{12} = \frac{\mathrm{I}_1}{\mathrm{V}_2} \Big| \mathrm{V}_1 = 0 \tag{2.24}$$

$$\mathrm{Y}_{21} = \frac{\mathrm{I}_2}{\mathrm{V}_1} \Big| \mathrm{V}_2 = 0 \qquad \mathrm{Y}_{22} = \frac{\mathrm{I}_2}{\mathrm{V}_2} \Big| \mathrm{V}_1 = 0 \tag{2.25}$$

In the reciprocity network, the equality $\mathrm{Z}_{12} = \mathrm{Z}_{21}$ and $\mathrm{Y}_{12} = \mathrm{Y}_{21}$ is valid. If it is symmetrical, the equality $\mathrm{Z}_{11} = \mathrm{Z}_{22}$ and $\mathrm{Y}_{11} = \mathrm{Y}_{22}$ are subtracted. In a lossless transmission network, the open-circuit impedance and short-circuit admittance parameters are completely virtual [15].

2.3.4. ABCD parameter

Microwave networks are easily characterized by S-, Z- and Y- matrices. In two-terminal networks, Z- and Y- matrices are used in series and in parallel. In practice, many filters and other components are expressed in serial steps. Therefore, it needs to be defined by ABCD or conduction (T-matrix). The ABCD matrix of a circuit block can be obtained from the product of several ABCD matrices of cascading two-terminal networks. In a two-terminal network, the representation of the voltage and current relations between terminals 1 and 2 by the ABCD matrix is as shown in Figure 2.11 and the mathematical expression is as in (2.18).

$$\begin{bmatrix} \mathrm{V}_1 \\ \mathrm{I}_1 \end{bmatrix} = \begin{bmatrix} \mathrm{A} & \mathrm{B} \\ \mathrm{C} & \mathrm{D} \end{bmatrix} \begin{bmatrix} \mathrm{V}_2 \\ \mathrm{I}_2 \end{bmatrix} \tag{2.26}$$

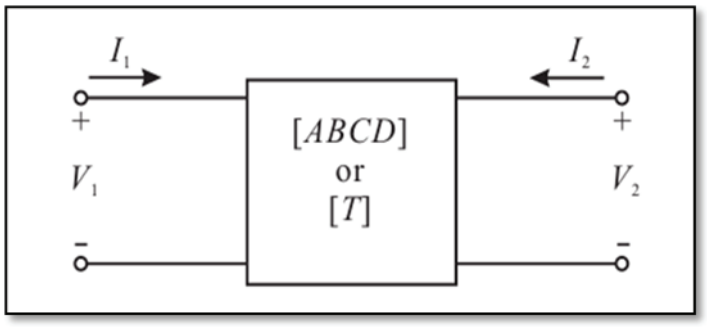


Figure 2.11. ABCD parameter representation

In the case where the circuit is symmetrical, the equality A = D is satisfied, while in the case where it has reciprocal properties, we obtain an equality of AD – BC = 1. In a lossless network, A and D are completely real, while B and C have only the virtual component. The input impedance of the circuit is shown in equation (2.19).

$$\mathrm{Z_{in}} = \frac{\mathrm{V_1}}{\mathrm{I_1}} = \frac{\mathrm{AZ_L + B}}{\mathrm{CZ_L + D}} \tag{2.27}$$

2.3.5. Transmission line network

The input impedance of two-gate networks can be defined as:

$$\mathrm{Z_{in1}} = \frac{\mathrm{V_1}}{\mathrm{I_1}} = \frac{Z_{02}\mathrm{A + B}}{\mathrm{Z_{02}C + D}} \tag{2.28}$$

If this equation is combined with the transmission line network, the following equation is obtained.

$$Z_{in1} = Z_c \frac{Z_{02} + Z_c \tanh \gamma l}{Z_c + Z_{02} \tanh \gamma l} \tag{2.29}$$

Z_c = Feature empedans

γ = Complex feed coefficient

l= Length of the transmission line

For a lossless environment, equality is provided, such as in Eq.(2.22).

$$Z_{in1} = Z_c \frac{Z_{02} + jZ_c \tan \beta l}{Z_c + jZ_{02} \tan \beta l} \tag{2.30}$$

In addition to these, it is equal to the value of two kinds of networks with a single terminal. This is followed by a terminal of a two-terminal transmission line that becomes an open-circuit or short-circuit [15].

$$Z_{in1}|z_{02=\infty} = \frac{A}{C} = \frac{Z_c}{\tanh \gamma l} \tag{2.31}$$

$$Z_{in1}|z_{02=0} = \frac{A}{C} = Z_c \tanh \gamma l \tag{2.32}$$

When it is lossless,

$$Z_{in1}|z_{02=\infty} = \frac{Z_c}{j\tan \beta l} \tag{2.33}$$

$$Z_{in1}|z_{02=0} = jZ_c \tan \beta l \tag{2.34}$$

2.4. Microstrip Lines and Components

Microstrip lines are specific paths that carry high-frequency electromagnetic waves and operate at millimeter wavelengths. These lines are used in many places in RF and microwave engineering applications. The lowest layer is the part consisting of soil. It has advantages such as transmission at high frequencies, low signal loss over long distances, easy integration and simple production.

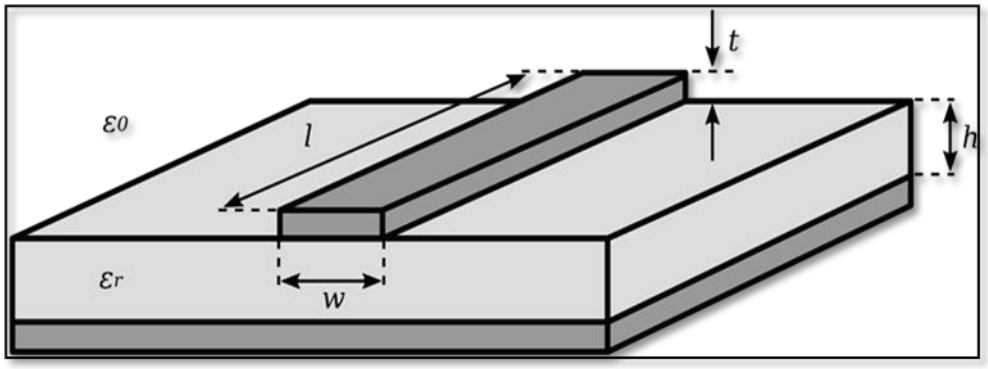


Figure 2.12. Microstrip transmission structure.

When creating the structures of microstrip filters, features such as bandwidths, size parameters and power consumption are examined.

We can see the structure of a microstrip in Figure 2.12. Here, we have a microstrip that has a width of *w* and a thickness of *t*. The line is located on a dielectric surface with a dielectric constant and thickness *h*. The lower part of the surface is a grounding plane, usually made

of copper. The areas in the microstrip have an inhomogeneous structure, with air at the top and dielectric at the bottom. Since this inhomogeneous structure prevents the microstrip from propagating a pure transverse electromagnetic (TEM) wave, the TEM wave has only transverse components and the propagation speed depends only on the material properties. The dielectric surface and the air, which form two different media, create electric and magnetic fields of the waves. Therefore, the propagation rate of the waves in the microstrip line also depends on the physical dimensions of the materials [10].

2.4.1. Effective dielectric constant and characteristic impedance

In the semi-TEM approach, the inhomogeneous dielectric-air medium in the microstrip is replaced by a homogeneous dielectric material with an effective dielectric permeability.

The expressions of the effective dielectric constant and wave impedance values are expressed by the following equations with the inferences in [16-17].

For $W/h \leq 1$

$$\varepsilon_{re} = \frac{\varepsilon_r+1}{2} + \frac{\varepsilon_r-1}{2}\{(1+12\frac{h}{W})^{-0.5}+0.04(1-\frac{W}{h})^2\} \quad (2.35)$$

$$Z_c = \frac{120\pi}{2} + \ln(\frac{8h}{W}+0.25\frac{W}{h}) \quad (2.36)$$

For $W/h \geq 1$

$$\varepsilon_{re} = \frac{\varepsilon_r+1}{2} + \frac{\varepsilon_r-1}{2}(1+12\frac{h}{W})^{-0.5} \quad (2.37)$$

$$Z_c = \frac{120\pi}{2} + \ln(\frac{8h}{W}+0.25\frac{W}{h}) \quad (2.38)$$

W/h Its approximate value and in terms are expressed as follows $Z_c\varepsilon_r$ $W/h \leq 2$

$$\frac{W}{h} = \frac{8\exp(A)}{\exp(2A)-2} \quad (2.39)$$

$$A = \frac{Z_c}{60}\{\frac{\varepsilon_r+1}{2}\}^{0.5} + \frac{\varepsilon_r-1}{\varepsilon_r+1}(0.23+\frac{0.11}{\varepsilon_r})^{-0.5}$$

$$\frac{W}{h} = \frac{2}{\pi}\left\{(B-1) - \ln(2B-1) + \frac{\varepsilon_r - 1}{2\varepsilon_r}\left[\ln(B-1) + 0.39 - \frac{0.61}{\varepsilon_r}\right]\right\} \quad (2.40)$$

$$B = \frac{60\pi^2}{Z_c\sqrt{\varepsilon_r}} \quad (2.41)$$

These statements provide much more accuracy than one percent. If more precise values are required, repetition or optimization processes can be carried out.

2.4.2. Directed wavelength propagation constant

After calculating the effective dielectric constant of the microstrip line, the directed wavelength of the semi-TEM mode is calculated at Eq.(2.42).

$$\lambda_g = \frac{\lambda_0}{\sqrt{\varepsilon_{re}}} \quad (2.42)$$

Where λ_0 represents the wavelength of empty space at the operating frequency. In relation to these, the propagation constant (β) and phase velocity ($\vartheta_{p)}$ calculation are made as follows.

$$\beta = \frac{2\pi}{\lambda_g} \quad (2.43)$$

$$\vartheta_p = \frac{w}{\beta} = \frac{c}{\sqrt{\varepsilon_{re}}} \quad (2.44)$$

Where c is the speed of light in empty space (c≈ 3.0 ×10^8 m/s). The electrical length of the line with a physical length l is in the form of equality (2.45).

$$\theta = \beta l \quad (2.45)$$

When $l = \frac{\lambda_g}{4}$ equals, when $\theta = \frac{\pi}{2}$, $l = \frac{\lambda_g}{2}$ = equals $\theta = \pi$.

2.5. Filter Design Methods

In filter designs, features such as slope ratio, return loss and interference loss in the suppression zone are important in the design. In addition, today, the fact that filters have

features such as more compact, cost-effective, and small size affects their physical parameters. There are basically two ways used in filter designs. Image parameters method and insertion loss method. These structures are converted into parts in the transmission line and used for filter design.

2.5.1. Image parameter method

The image parameters method for filter design includes simple two-terminal cascade band-pass and band-stop. This method is quite simple, but random frequency responses cannot be included in the filter. It provides a link between practical filter designs and infinite periodic structures.

In Figure 2.13;

Zi1 = Input impedance at terminal 1 when terminal 2 is terminated by Z_{i2}.

Zi2 = Input impedance at terminal 2 when terminal 1 is terminated by Z_{i1}.

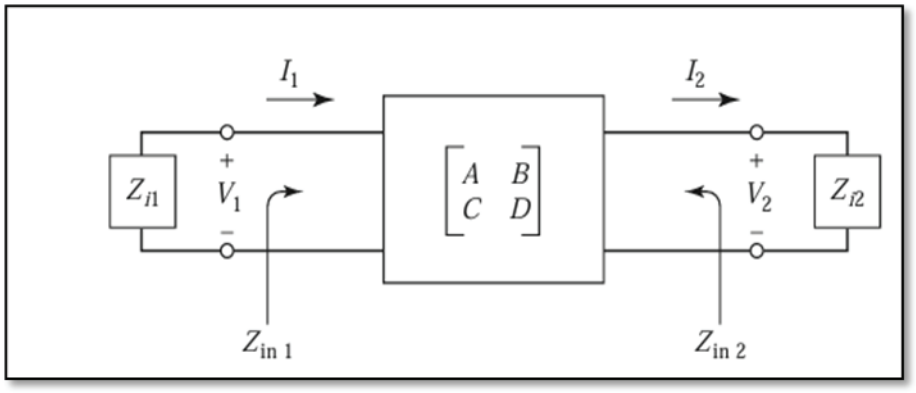


Figure 2.13. Two-Port ABCD matrix

Both terminals match their image impedances. We can express image impedances in terms of ABCD parameters, as in Eq.(2.46) [6].

$$Z_{i1} = \sqrt{\frac{AB}{CD}} \tag{2.46}$$

2.5.2. Insertion loss method

A perfect filter should have zero insertion loss in the bandpass region, infinite attenuation in the stop zone, and a linear response, but this is not possible in real life. The insertion loss

method has high control and phase characteristic in the bandpass and stop region in a systematic way for the desired frequency response. Some applications are available according to the required design requirements. For example, if low insertion loss is at the forefront, the binomial method is used, and if a sharp cutting frequency is preferred, the Chebyshev design method is used. As the degree of the filter is increased, its performance is changed.

In the insertion loss method, a filter response is defined by its insertion loss or power loss rate, P_{LR}.

$$P_{LR} = \frac{P_{inc}}{P_{load}} = \frac{1}{1-|\Gamma(w)|^2} \tag{2.47}$$

Insertion Loss (IL) is expressed in dB as in Eq.(2.37).

$$\text{IL} = 10 \log P_{LR} \tag{2.48}$$

$|\Gamma(w)|^2$w is a double function of and can be expressed as a polynomial of w^2.

$$|\Gamma(\text{w})|^2 = \frac{\text{M}(\text{w}^2)}{\text{M}(\text{w}^2)+\text{N}(\text{w}^2)} \tag{2.49}$$

M and N are also real polynomials. This gives us the following equality.

$$\text{P}_{\text{LR}} = 1 + (2.39)\frac{\text{M}(\text{w}^2)}{\text{N}(\text{w}^2)} \tag{2.50}$$

In order to be a physically feasible filter, the power loss ratio must be the same as .The process of designing a filter with the insertion loss method is as shown in Figure 2.14.

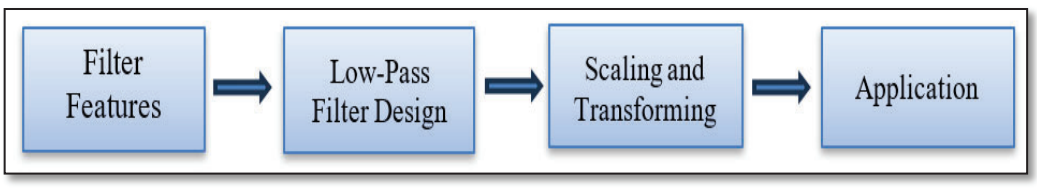


Figure 2.14. General filter design process block

I. Maximum flatness (Binomial or Butterworth) filter approach

This characteristic filter structure gives the straightest frequency response in the bandpass region. The power loss parameter for a low-pass filter can be written as follows.

$$P_{LR} = 1 + k^2 \left(\frac{w}{w_c}\right)^{2N} \quad (2.40)$$

Where;
N = Degree of filter
w_c= Cut-off Frequency

The band-pass part w_c expands from w to a, and the power loss ratio at the belt corners is $1+k^2$. If the -3dB point is selected, k=1. If $w > w_c$ the attenuation gradually increases with the frequency, as shown in Figure 2.15.

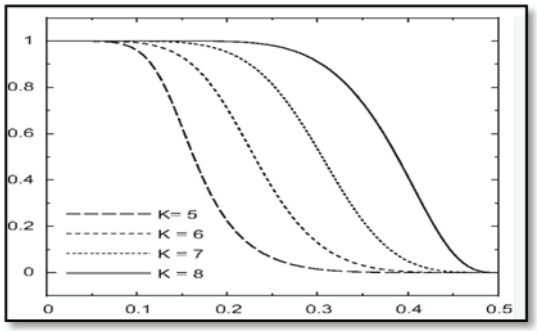


Figure 2.15. Maximum flat filter chart

In case of w >> w_c

$$P_{LR} \cong k^2 \left(\frac{w}{w_c}\right)^{2N} \quad (2.51)$$

equalization occurs, and the insertion loss increases by 20N dB/decade.

II. Equal Fluctuation (Chebyshev) Filter Approach

If we customize the insertion loss of a filter that passes lower than the n^{th} order using the Chebyshev polynomial, we get the Eq. (2.52).

$$P_{LR} = 1 + k^2 T_N^2 \left(\frac{w}{w_c}\right) \quad (2.52)$$

Even if there are fluctuations of $1+k^2$ in the band-pass region, a sharper cut is obtained (Figure 2.16).

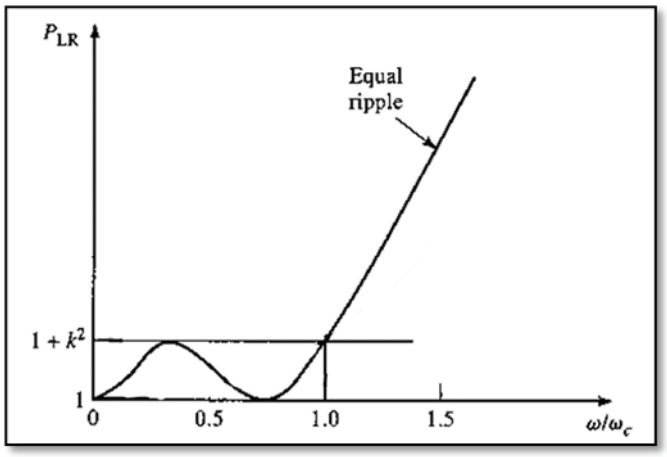


Figure 2.16. Chebyshev low-pass 3rd order filter response

In the case of w >>w_c, the insertion loss is simplified as follows.

III. Elliptic function filter approach

The Maximum Flatness and Equal Ripple responses both have monotonically increasing attenuation in the band-stopping region. In many applications it is sufficient for minimum belt stopping but for a better cutting ratio Elliptic functions are preferred. These have an equal ripple response in the band-stopping region in addition to the band-stop region.

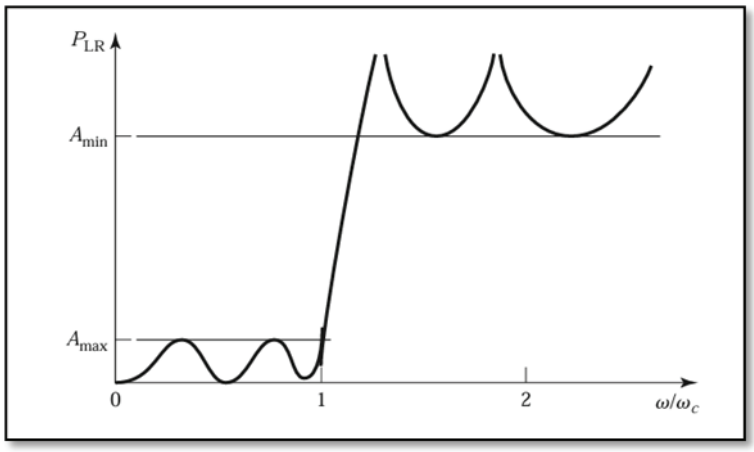


Figure 2.17. Elliptic filter frequency response

IV. Linear phase filter approach

The linear phase approximation is a design method that ensures that the frequency response of a microwave filter is smooth and linear, especially in terms of group latency. In linear phase filters, the differences between the phases of signals of different frequencies are kept to a minimum. This preserves the phase harmony of the signals passing through the filter. This property is often important in signal processing and transmission applications because signals can be processed or transmitted without breaking the phase harmony.

$$\emptyset(\mathrm{w}) = \mathrm{Aw}\left[1 + \mathrm{p}\left(\frac{\mathrm{w}}{\mathrm{w_c}}\right)^{2\mathrm{N}}\right] \tag{2.53}$$

Where; $\emptyset(\mathrm{w})$ is the phase of the voltage transfer function of the filter, p is a constant. The group delay associated with this is expressed as in Eq. (2.54).

$$\tau_d = \frac{d\emptyset}{dw} = \mathrm{A}\left[1 + \mathrm{p}(2\mathrm{N}+1)\left(\frac{\mathrm{w}}{\mathrm{w_c}}\right)^{2\mathrm{N}}\right] \tag{2.54}$$

2.6. Filter Transformations and Application

In low-pass filters, we have normalized designs where the source frequency is 1 and the cut-off frequency is $\Omega w_c = 1$ rad/sec. We can achieve high-pass, band-pass and band-stop filters by changing their frequency and impedance. The converted elements perform well for low frequencies in bulk element filter designs, but some problems arise at high and RF

frequencies. Batch-element inductors and capacitors are difficult to implement at microwave frequencies.

2.6.1. Frequency and impedance scaling

In impedance scaling, in the prototype design, the welding and load resistors are one unit and the welding impedance (R_0) is obtained by multiplying by all impedances. The new components are the same as in equality.

$$L' = R_O L\ ,\ C' = \frac{C}{R_O}\ , R_S{}' = R_O\ , R_L{}' = R_O R_L \tag{2.55}$$

Where; L, C and R_L are the original components. Frequency scaling, on the other hand, is done by converting the cut-off frequency from unit to.

$$w \leftarrow \frac{w}{w_c}$$

The new power loss ratio is the same as in Eq.(2.56).

$$P'_{LR}(w) = P_{LR}(\frac{w}{w_c}) \tag{2.56}$$

Frequency and impedance scaling for low-pass and high-pass filter are as shown Figure 2.18.

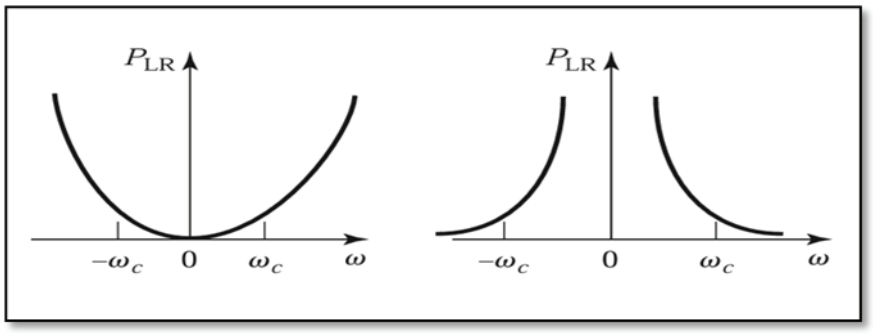


Figure 2.18. Frequency and impedance scaling for low-pass and high-pass filter

When impedance and frequency scaling are applied together, equality is obtained for the low pass:

$$L'_k = \frac{R_O L_k}{w_c} \quad (2.57)$$

$$C'_k = \frac{C_k}{R_O w_c} \quad (2.58)$$

The low-pass filter prototype bandpass and band-stop transformations are as shown in Figure 2.19. If there are corners of the and band-passing section, following equations are achieved.

$$w \leftarrow \frac{w_0}{w_2 - w_1}\left(\frac{w}{w_0} - \frac{w_0}{w}\right) = \frac{1}{\Delta}\left(\frac{w}{w_0} - \frac{w_0}{w}\right) \quad (2.59)$$

$\Delta = \frac{w_2 - w_1}{w_0} \rightarrow$ Fractional Bandwidth

$w_0 = \sqrt{w_1 w_2} \rightarrow$ Center Frequency

The series inductor circuit turns into a series LC circuit, and the parallel capacitor circuit turns into a parallel LC circuit.

Equation for series inductor:

$$L'_k = \frac{\Delta L_k}{w_0} \quad (2.60)$$

$$C'_k = \frac{1}{w_0 L_k} \quad (2.61)$$

Equation for Parallel Capacitor:

$$L'_k = \frac{1}{w_0 \Delta C_k} \quad (2.62)$$

$$C'_k = \frac{\Delta C_k}{w_0} \quad (2.63)$$

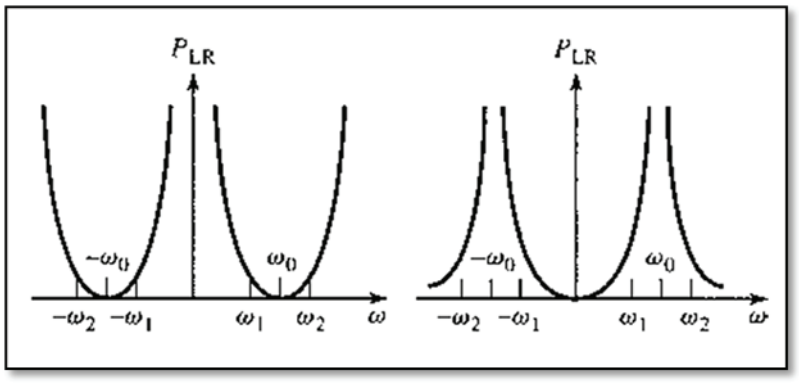


Figure 2.19. Bandpass and bandstop conversions

Transformations for all filter states are shown in Table 2.1.

Table 2.1 Filter Transform

Low-pass	High-pass	Band pass	Bandstop
L	$\frac{1}{\omega_c L}$	$\frac{L}{\omega_0 \Delta}$ $\frac{\Delta}{\omega_0 L}$	$\frac{L\Delta}{\omega_0}$ $\frac{1}{\omega_0 L\Delta}$
C	$\frac{1}{\omega_c C}$	$\frac{\Delta}{\omega_0 C}$ $\frac{C}{\omega_0 \Delta}$	$\frac{1}{\omega_0 C\Delta}$ $\frac{C\Delta}{\omega_0}$

2.6.2. Richard's transformations

As a frequency conversion technique, it is used in circuit design to change the desired properties in another frequency band while preserving them. These transformations make Sparameters using a set of transformation functions as frequency-independent variables. These transformations are used to reduce unwanted frequency responses. It transforms from

the W plane to the plane that repeats with periods [18].

$$\Omega = tan\beta l = tan\left(\frac{wl}{\vartheta_p}\right) \tag{2.64}$$

$$jX_L = j\Omega L = jLtan\beta l \tag{2.65}$$

$$jB_C = j\Omega C = jCtan\beta l \tag{2.66}$$

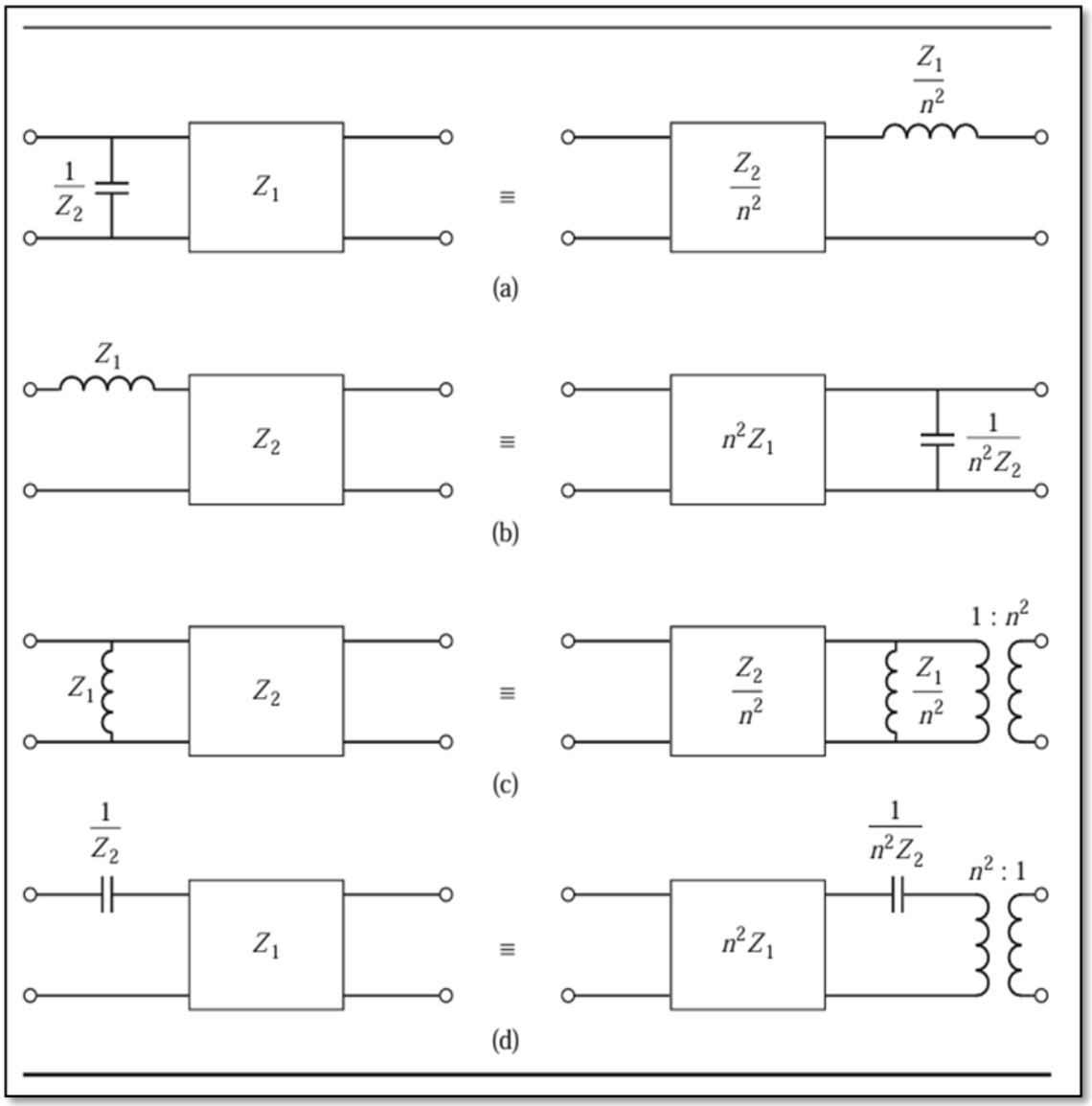
The short circuit in the inductor length and with the characteristic impedance can be displaced by the stud. In the same way, an open circuit in the capacitor can be replaced by a stud. The cut-off frequency for the low-pass filter prototype is one unit. In order to obtain the same cut-off frequency, the equality in (2.67) must be achieved.

$$\Omega = 1 = tan\beta l \tag{2.67}$$

2.6.3. Kuroda identities

In the design of microstrip lines of bandpass filters, the filter elements are physically separated by the transmission line sections. Kuroda identities determine the impedances of the microstrip lines of the bands that are equivalent in the opposite sense. These equations ensure that the bandpass filters on the microstrip line work in a balanced manner. These equations, which are used to determine filter properties in a specific frequency range, help determine the widths, lengths, and other parameters of microstrip lines. The fact that microstrip lines simplify their complex interactions is the benefit of Kuroda equations. This simplifies filter design. In Table 2.2 we can find all the transformations.

Table 2.2. Equality of the Four Kuroda



3. DESIGN AND MANUFACTURE OF BANDPASS FILTER

Microstrip bandpass filters are the structures that passes the signals in the desired band range and tries to suppress the signal in the other parts. Filters gain features according to specific purposes. These are important parameters such as cutting frequency, center frequency, pressure ratio, return loss rate, insertion loss rate. The aim of this thesis is to create a new band-pass filter after parameter calculations are made in accordance with the frequencies used in 5G applications.

The frequency values requested in 5G applications were investigated 3.5 GHz center frequencies were taken. Filter types were examined and the Butterworth frequency response technique was chosen because it does not cause fluctuations. Compared to other previous studies, a more compact structure has been obtained. Dimensionally, it is reduced compared to the standard parallel coupling structure.

In the filter design, a low-pass filter circuit is first installed in accordance with the requirements.

These values with the desired values are converted into the L-C circuit. Our source supply and output part are calculated to be 50 ohms. In the next step, these values are created in a band-pass filter circuit using the filter transformations technique. In order to create the microstrip transmission structure of the filter, the Richard transformation and the Kuroda equations are used to transform it into a distributed element structure.

Various methods are used to evaluate filter performance and study its characteristic structures. Methods such as Transfer Function, Attenuation factor, S-Parameters, ABCD Matrix. In this study, S-parameters were taken as a basis and the attenuation properties with filter pass band were examined using the S21 parameter.

ADS program was used for filter design, LC circuit design and optimization. CST program was used for 3D design, electromagnetic analysis and examination of filter results.

3.1. Parallel Coupling 3.5 GHz Bandpass Filter Design

3.1.1. Butterworth low-pass LC filter prototype

A 300 MHz bandwidth with a 4th order band pass operating at 3.5 GHz and a cut-off frequency of 3350 MHz and 3650 MHz was selected. In this study, a new design is proposed to change the known parallel coupling bandpass filter structure.

Similar results were observed by bending 90 degrees from half of the filter to gain the overall size of the filter. FR-4 was preferred as the substrate material in the filter design. The height h and copper thickness *t* of this insulating base material are preferred. The dielectric constant of FR-4 material is $\varepsilon_r = 4.3$, $h = 0.8$ mm, $t = 0.035$ mm.

Table 3.1. Filter Properties

Properties	Value
Center Frequency	3.5 GHz
Bandwidth	300 MHz
Low-Pass Prototype	Butterworth
Filter Degree	4
I/O Empedansı	50 ohms
S_{11} and S_{21} Values	S_{11}<-30 dB S_{21}>-3 dB

In determining the degree of filter, the degree is determined on the Butterworth attenuation normalized frequency graph according to the requirements.

f_a=3.350 GHz, f_b=3.650 GHz, f_0= 3.5 GHz, f_c=3.7 GHz

$$f_0 = \sqrt{f_a x f_b} = 3.49.10 \text{ GHz} \quad (3.1)$$

$$FBW = \frac{f_b - f_a}{f_0} = 0.085 \quad (3.2)$$

$$f_n = \frac{1}{FBW} x \left(\frac{f_a}{f_c} - \frac{f_c}{f_a}\right) = -2.35 \quad (3.3)$$

Normalize Frequency $\left|\frac{f_n}{1}\right|$-1=1.35 (3.4)

Where;

The value we found was selected as 4 for the filter degree from the graph in Figure 3.1.

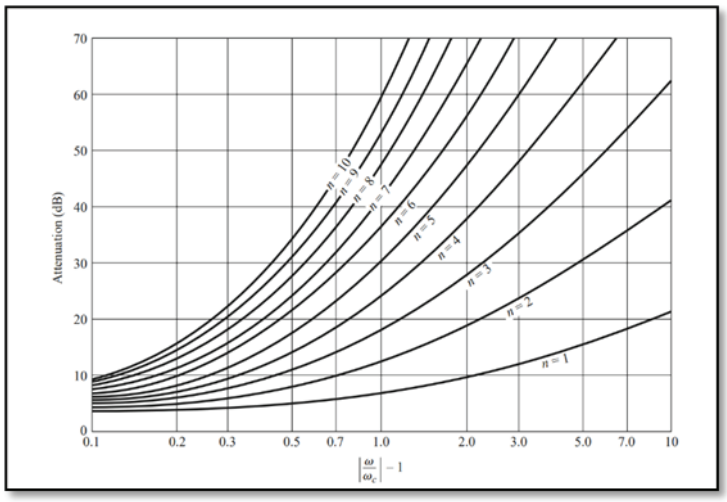


Figure 3.1. Butterworth normalized frequency attenuation graph

3.1.2. 4th Degree low pass filter design and band-pass filter design

After the filter degree is determined, the values used in the filter are determined from Table 3.2.

Table 3.2. Butterworth Low-Pass Filter Values

N	g_1	g_2	g_3	g_4	g_5	g_6	g_7	g_8	g_9	g_{10}	g_{11}
1	2.0000	1.0000									
2	1.4142	1.4142	1.0000								
3	1.0000	2.0000	1.0000	1.0000							
4	0.7654	1.8478	1.8478	0.7654	1.0000						
5	0.6180	1.6180	2.0000	1.6180	0.6180	1.0000					
6	0.5176	1.4142	1.9318	1.9318	1.4142	0.5176	1.0000				
7	0.4450	1.2470	1.8019	2.0000	1.8019	1.2470	0.4450	1.0000			
8	0.3902	1.1111	1.6629	1.9615	1.9615	1.6629	1.1111	0.3902	1.0000		
9	0.3473	1.0000	1.5321	1.8794	2.0000	1.8794	1.5321	1.0000	0.3473	1.0000	
10	0.3129	0.9080	1.4142	1.7820	1.9754	1.9754	1.7820	1.4142	0.9080	0.3129	1.0000

According to the values obtained, the 4th degree Butterworth filter circuit is as shown in Figure 3.2. PI-network collective element circuit was preferred as the topology.

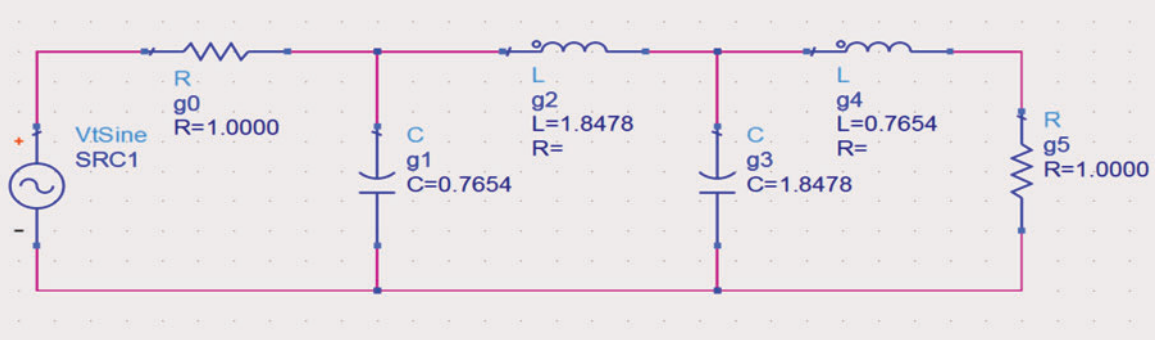


Figure 3.2. Prototype low-pass circuit of the 4th order

The input and output impedances of the circuit are selected as 50 ohms. By applying these values to the transformation formulas, the bandpass filter aggregate element values are obtained. In this conversion, the L (inductor) value in the parallel low pass becomes the series L and C (capacitance) values, while the parallel C value is converted to parallel L and parallel C values (Figure 3.3).

Fractional Bandwidth: $\Delta = \frac{w_1 - w_2}{w_0}$ (3.5)

$L' = \frac{L}{w_0 \Delta}$ $C' = \frac{\Delta}{w_0 L}$ (3.6)

$L' = \frac{\Delta}{w_0 C}$ $C' = \frac{C}{w_0 \Delta}$ (3.7)

When the values we have are put in their places and processed, the following results occur. All elements values are shown in Table 3.2.

$g_1 = 0.7654$ $g_2 = 1.8478$ $g_3 = 1.8478$ $g_4 = 0.7654$ $g_5 = 1.0000$

$Z_0 = 50$ ohm $f_1 = 3350$ MHz $f_0 = 3500$ MHz $f_2 = 3650$ MHz

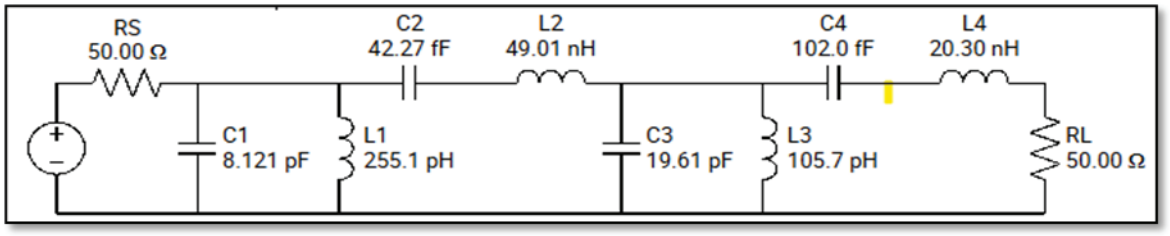


Figure 3.3. 4th degree bandpass filter circuit with bulk elements

Table 3.3. 4th Order Inductor and Capacitor Values

C_1	L_1	C_2	L_2	C_3	L_3	C_4	L_4
8.121 pF	255.1 pH	42.27 fF	49.01 nH	19.61 pF	105.7 pH	102.0 fF	20.30 nH

Admittance transducers play an important role in parallel-coupled bandpass filter designs (Figure 3.4). As a result of ABCD matrix solutions and analysis, the following formulas emerge.

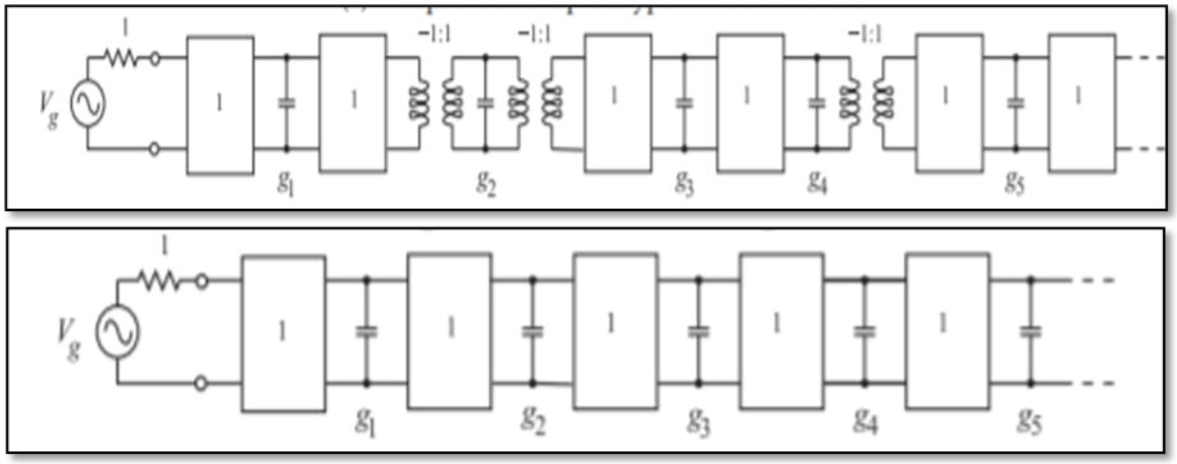


Figure 3.4. Bandpass filter admitance transducer

The intercoupling structure can be calculated from the following equations.

$$Z_0 J_1 = \sqrt{\frac{\pi}{2g_1}} \frac{\Delta w}{w_0} \tag{3.8}$$

$$Z_0 J_n = \frac{\pi}{2\sqrt{g_{n-1} g_n}} \frac{\Delta w}{w_0} \tag{3.9}$$

$$Z_0 J_{N+1} = \sqrt{\frac{\pi}{2g_N g_{N+1}}} \frac{\Delta w}{w_0} \tag{3.10}$$

The inverter response of each section is as follows:

$$Z_0 J_1 = \sqrt{\frac{\pi}{2\times 0.7654} \frac{300\ MHz}{3500\ MHz}} = 0.4192 \tag{3.11}$$

$$Z_0J_2 = \frac{\pi}{2\sqrt{0.7654\times1.8478}}\frac{300MHz}{3500\ MHz} = 0.1131 \quad (3.12)$$

$$Z_0J_3 = \frac{\pi}{2\sqrt{1.8478\times1.8478}}\frac{300MHz}{3500\ MHz} = 0.072 \quad (3.13)$$

$$Z_0J_4 = \frac{\pi}{2\sqrt{1.8478\times0.7654}}\frac{300MHz}{3500\ MHz} = 0.1131 \quad (3.14)$$

$$Z_0J_5 = \sqrt{\frac{\pi}{2\times0.7654}\frac{300\ MHz}{3500\ MHz}} = 0.4192 \quad (3.15)$$

Each coupling has Double and Single characteristic impedance. These impedance values will be used in the next step to derive the line width and gaps of the filter. According to the double and single mode impedance formula, the calculations are as follows.

$$Z0_{e1} = Z_0[1 + Z_0J_1 + (Z_0J_1)^2] = 50[1 + 0.4192 + (0.4192)^2] = 79.74\ \Omega$$

$$Z0_{01} = Z_0[1 - Z_0J_1 + (Z_0J_1)^2] = 50[1 - 0.4192 + (0.4192)^2] = 37.82\ \Omega$$

$$Z0_{e2} = Z_0[1 + Z_0J_1 + (Z_0J_1)^2] = 50[1 + 0.4192 + (0.4192)^2] = 56.30\ \Omega$$

$$Z0_{02} = Z_0[1 + Z_0J_1 + (Z_0J_1)^2] = 50[1 - 0.4192 + (0.4192)^2] = 44.98\ \Omega$$

$$Z0_{e3} = Z_0[1 + Z_0J_1 + (Z_0J_1)^2] = 50[1 + 0.4192 + (0.4192)^2] = 53.85\ \Omega$$

$$Z0_{03} = Z_0[1 + Z_0J_1 + (Z_0J_1)^2] = 50[1 - 0.4192 + (0.4192)^2] = 46.65\ \Omega$$

$$Z0_{e4} = Z_0[1 + Z_0J_1 + (Z_0J_1)^2] = 50[1 + 0.4192 + (0.4192)^2] = 56.30\ \Omega$$

$$Z0_{04} = Z_0[1 + Z_0J_1 + (Z_0J_1)^2] = 50[1 - 0.4192 + (0.4192)^2] = 44.98\ \Omega$$

$$Z0_{e5} = Z_0[1 + Z_0J_1 + (Z_0J_1)^2] = 50[1 + 0.4192 + (0.4192)^2] = 79.74\ \Omega$$

$$Z0_{05} = Z_0[1 + Z_0J_1 + (Z_0J_1)^2] = 50[1 - 0.4192 + (0.4192)^2] = 37.82\ \Omega$$

The parallel coupling bandpass filter values are shown in Table 3.4.

Table 3.4. Parallel Coupling Bandpass Filter Values

Coupling Step	Admitance İnverter	Even Mode Impedance Z_e	Odd Mode Impedance Z_0
1	0.4192	79.74	37.82
2	0.1131	56.30	44.98
3	0.072	53.85	46.65
4	0.1131	56.30	44.98
5	0.4192	79.74	37.82

3.1.3. Dimensional calculations of bandpass microstrip filter

In this design, the material FR-4 with a dielectric constant is chosen. Substone materials are of great importance in terms of production cost and accuracy of results in filters. As the filter size increases, it can be designed with materials with smaller dielectrics. The most important feature of FR-4 material is that it is flame retardant and can be easily found in the market. It is frequently used in circuit boards because it has fairly good electrical properties. For this material, it is preferred to be used as copper thickness, which is one of the standard transmission heights. According to the data obtained in Table 3.4 and the material properties, the length, width and gap structures of each coupling part are calculated. The results of the dimensional parameters are obtained by calculations made in the ADS program based on the obtained data, as in Table 3.5. $\varepsilon_r = 4.3, h = 0.8\ \text{mm}, t = 0.035\ \text{mm}$.
Size calculation for 50 ohm supply lines;

$Z_0 = 50 \quad \varepsilon_r = 4.3 \quad h = 0.8$

$\frac{w}{h} < 2$;

$$A = \frac{Z_c}{60} \times \sqrt{\frac{(e_r+1)}{2}} + \frac{(e_r-1)}{(e_r+1)} \times \left(0.23 + \frac{0.11}{e_r}\right) = 1.3825 \qquad (3.16)$$

$$\frac{w}{h} = \frac{8 \times e^{A}}{e^{2A}-2} = 2.2225 \quad (3.17)$$

$$w = \frac{w}{h} \times h = 1.568 \quad (3.18)$$

$$\frac{w}{h} > 2;$$

$$B = 377 \times \frac{\pi}{2 \times Z_0 \times \sqrt{e_r}} = 5.4053 \quad (3.19)$$

$$\frac{w}{h} = \frac{2}{\pi} \times \left(B - 1 - \ln(2 \times B - 1) + \left(\frac{e_r - 1}{2e_r}\right) \times \left(\ln(B-1) + 0.39 - \frac{0.61}{e_r} \right) \right) = 2.2185 \quad (3.21)$$

Wavelength calculation for 50 ohms;

$$\lambda = \frac{c}{f \times e_r} \qquad c = 3 \times 10^{8} \;, \quad f = 3.5 \times 10^{6} \;, \quad e_r = 4.8$$

$$e_f = \frac{e_r + 1}{2} + \frac{e_r - 1}{2} \times (1 + 12 \times \frac{h}{w})^{-\frac{1}{2}} = 3.546 \quad (3.20)$$

$$\lambda = \frac{c}{f \times \sqrt{e_f}} = 45.59 \quad (3.21)$$

$$L = \frac{\lambda}{4} = 11.4\, mm \quad (3.22)$$

The dimensional parameters in Table 3.5 are obtained directly without long calculations through the ADS program (Figure 3.5).

Table 3.5. Calculated Filter Dimensional Parameters

Line Structure	W (mm)	S (mm)	L (mm)
Feeding Line	1.55	-	11.6
Coupling Line 1	1.00	0.12	12.3
Coupling Line 2	1.55	0.88	11.6
Coupling Line 3	1.80	1.55	11.6
Coupling Line 4	1.55	0.88	11.6
Coupling Line 5	1.00	0.12	12.3

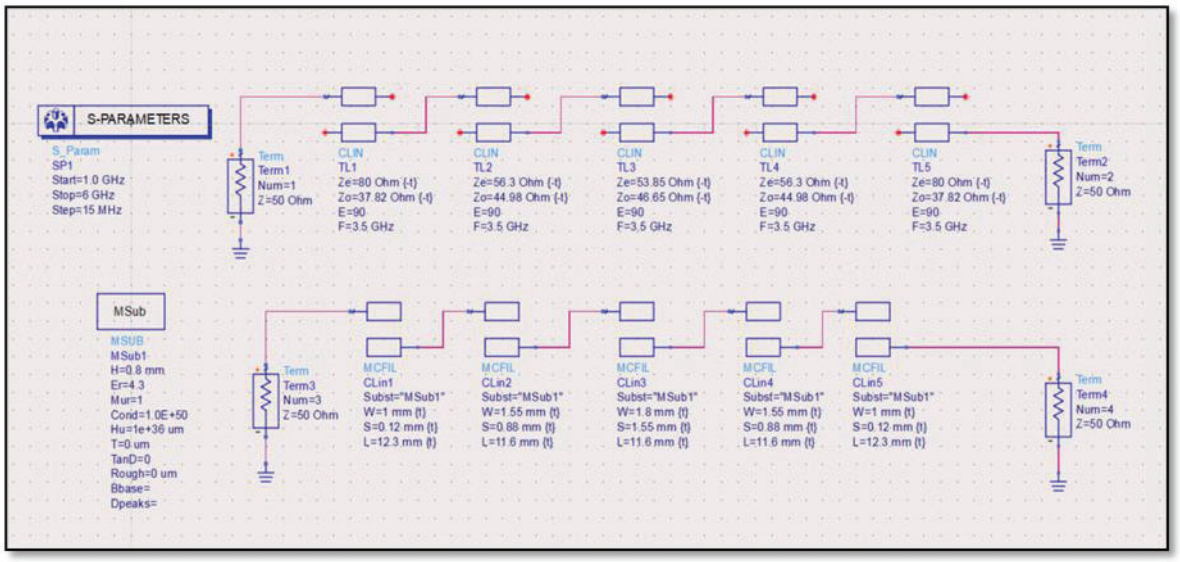


Figure 3.5. 4th order bandpass filter ads dimensional calculations

The filter, all of whose values are calculated, is drawn through the CST program. A new structure has been obtained by changing the standard parallel coupling structure (Figure 3.6).

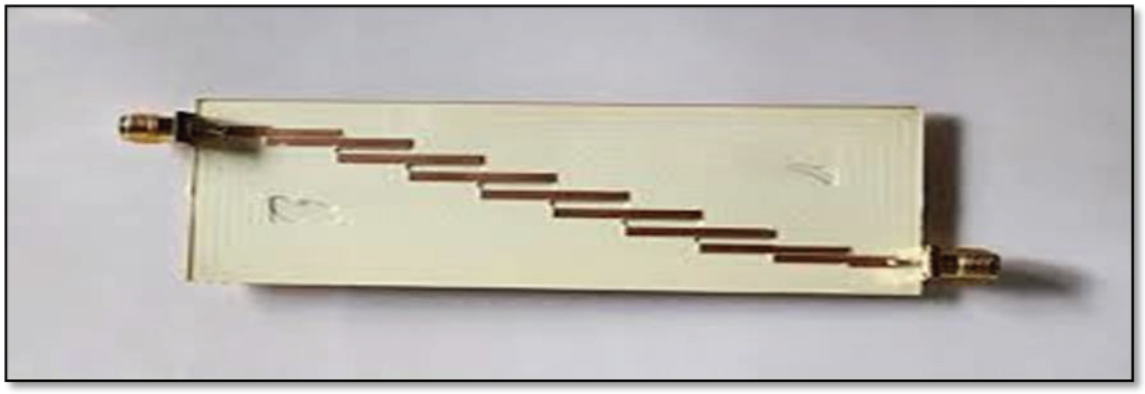


Figure 3.6. Standard parallel coupling bandpass filter structure

Since it is desired to pass a signal in a certain range in band-pass filters, a design is made accordingly. In this design (Figure 3.7), it was determined as 300 MHz, and other parameters were calculated based on it. As shown in Figure 3.8, a bandwidth of 300 MHz has been captured. The cut-off frequencies are 3.4 GHz and 3.7 GHz points. These points are where the signal drops by -3dB. Since they are symmetrical circuits, the values of and are the same. $|S_{11}| = |S_{22}|$ and $|S_{12}| = |S_{21}|$.

Table 3.6. Optimized Dimensional Values

Line Description	Calculated Filter Dimensions			Optimised filter sizes		
	W (mm)	S (mm)	L (mm)	W (mm)	S (mm)	L (mm)
Coupling Line 1	1.17	0.16	12	1	0.12	12.3
Coupling Line 2	1.85	0.8	11.7	1.55	0.88	11.6
Coupling Line 3	2	1.18	11.7	1.8	1.55	11.6
Coupling Line 4	1.85	0.8	11.7	1.55	0.88	11.6

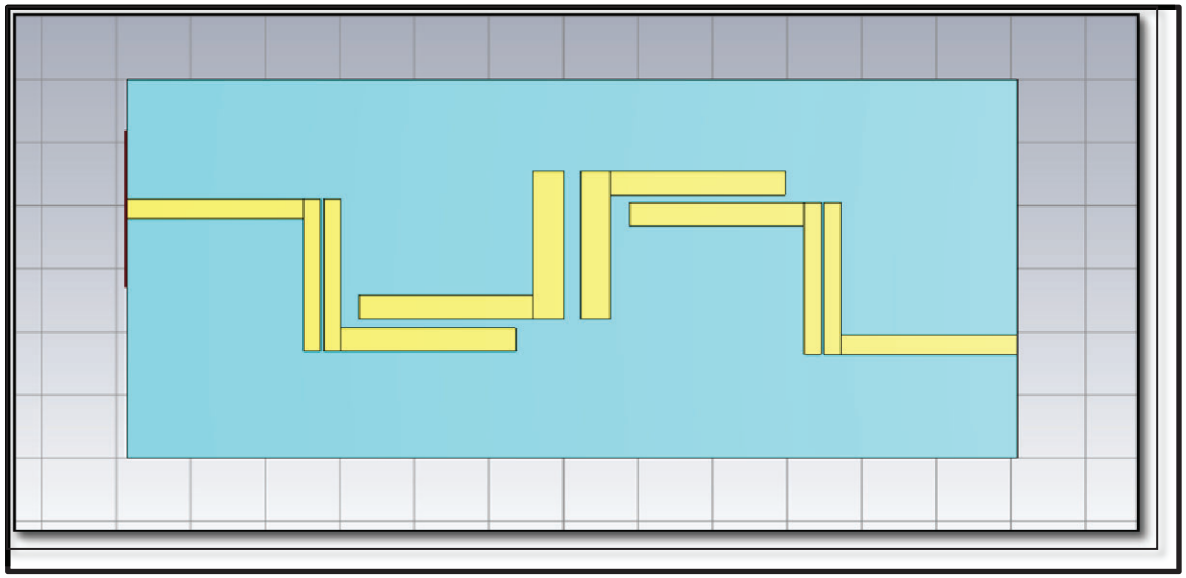


Figure 3.7. Recommended bandpass filter structure

The results of the design drawn in CST were compared with the results of the ADS program. It has been optimized by making corrections to the parameters through the design (Table 3.6). In the first results, the bandwidth of the filter was less than 300 MHz and the center frequency was near 3.6 GHz. After optimization, the answer of the filter was obtained as shown in Figure 3.8. It is seen that the return loss value S_{11} is -30.33 dB and the insertion loss value S_{21} is -0.73 dB at the center frequency.

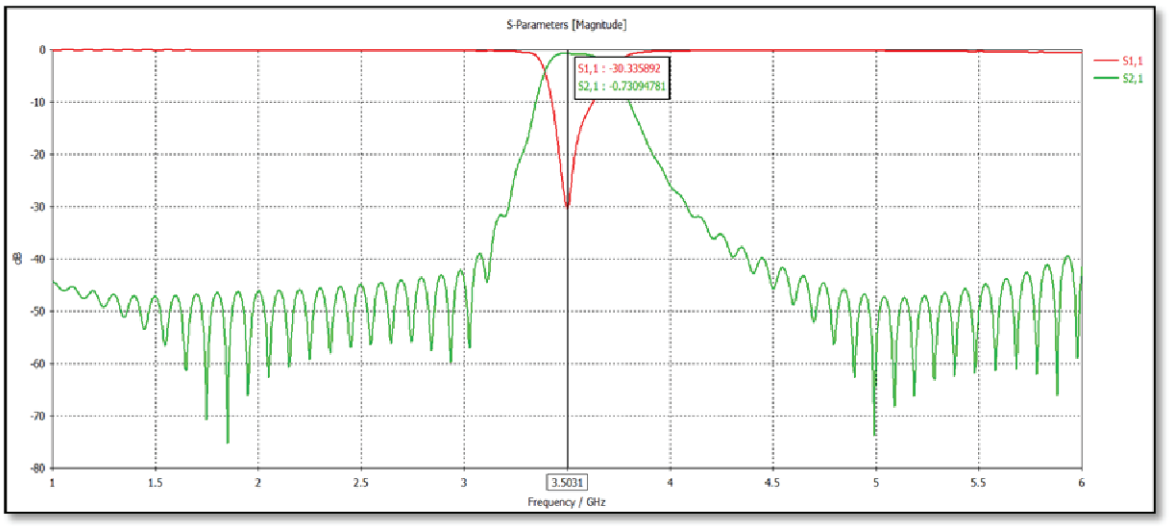


Figure 3.8. Bandpass filter s_{11} and s_{21} results

The results of the filter S_{11}, S_{21} were quite good. The closer our insertion loss value is to zero, the better our signal will pass in that region. Conversely, our return loss is expected to be less than -10 dB. These regions are our passing areas (Figure 3.9). In the signal stop regions of our filter, it is seen that our value is generally below -40 dB and at most 1.7 GHz it is around -85 dB. This leads us to conclude that a good stop has been made in unwanted areas.

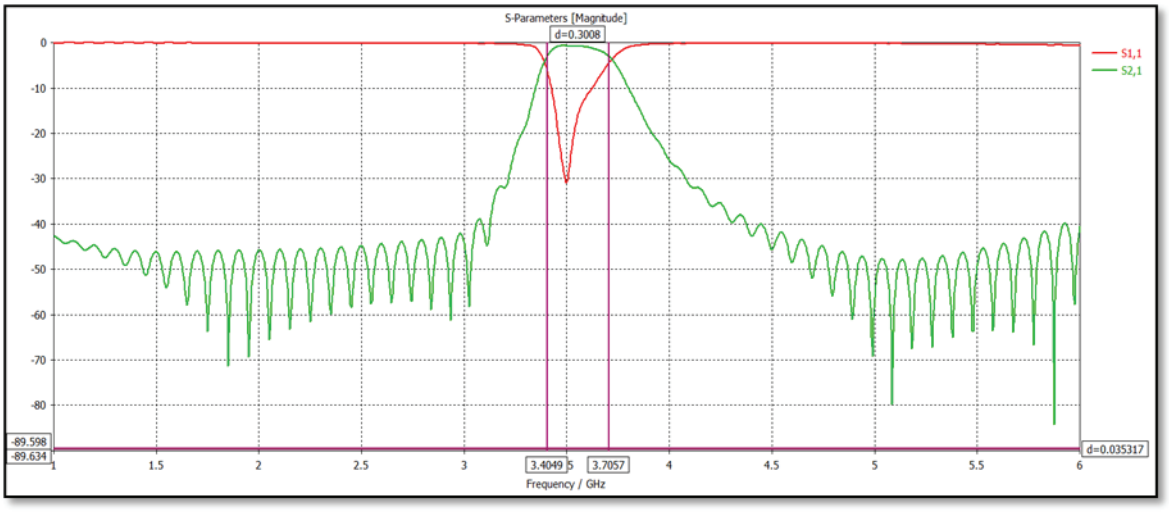


Figure 3.9. Bandwidth graph of the bandpass filter

Another important parameter that affects filter performance is group latency. It refers to what is the phase difference between the various frequency components. An ideal group delay should be in the form of a horizontal line. In bandpass filters, where there is signal crossover,

it should be between 0 and 5. In this study, the group lag results can be seen from the graph in Figure 3.10. The group delay of the bandpass filter is at the desired level in the specified frequency range.

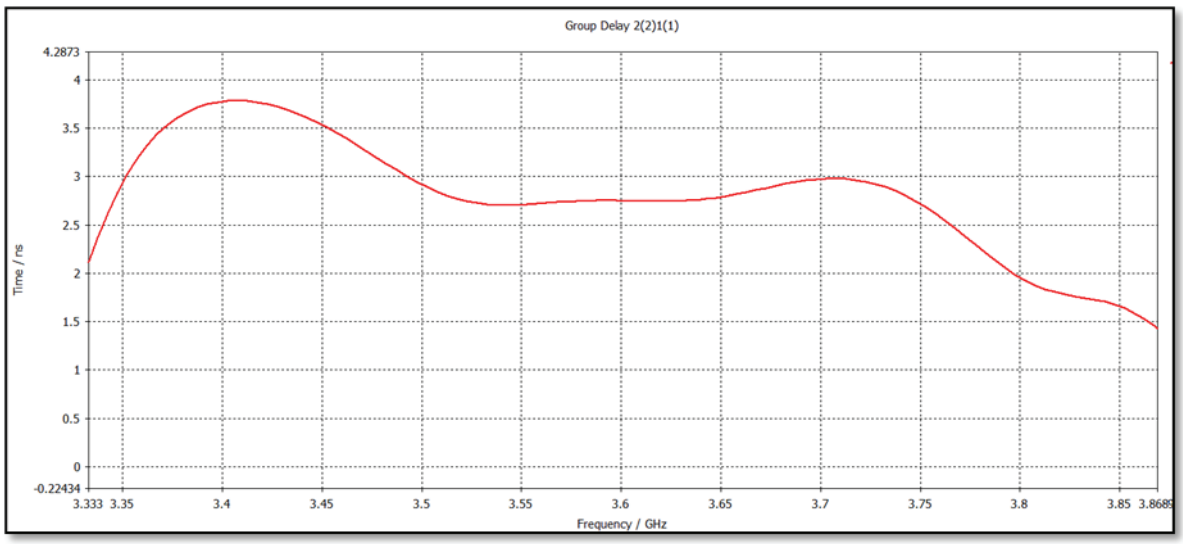


Figure 3.10. Bandpass filter group latency graph

Figure 3.11 shows the results of the filter's surface current distribution at 3.5 GHz. Surface currents indicate at which frequency the signal is more intense on the filter.

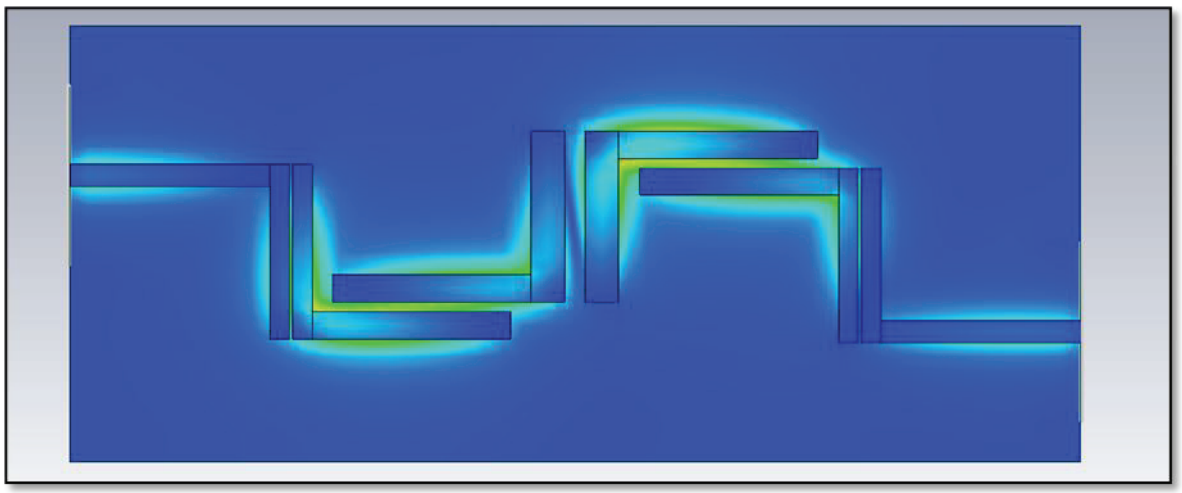


Figure 3.11. Bandpass filter surface current distribution

A comparison of similar parallel coupling structures made earlier is given in Table 3.7.

Table 3.7. Comparison of Similar Studies

Return Loss (S11)	Insertion Loss (S21)	Bandgap	Dimensions	Substone Material	Referenc e
-25 dB	-0.1 dB	2.4 GHz-3.6 Ghz	9,6 cm x 4.6 cm	AD600	[24]
-20 dB	-1.79 dB	2.96 GHz-3.140 GHz	5.6 cm x 5.5 cm	Duroid 5880	[25]
-12 dB	-0.49 dB	2.92 GHz-10.95 GHz	10.9 cm x 7.59 cm	AD260A	[26]
-17.3 dB	-2.2 dB	3.35 GHz - 4.5 GHz	6 cm x 3 cm	FR-4	[27]
-30 dB	-0.1 dB	2.5 GHz - 3.2 GHz	6 cm x 6 cm	F4BM	[28]
-31 dB	-0.75 dB	3.4 GHz -3.7 GHz	6 cm x 3 cm	FR-4	Thesis Study

3.2. Production and Measurement of the Designed 3.5 GHz Bandpass Filter

It was decided to produce the 4th order Butterworth 3.5 GHz bandpass filter, from which the simulation results were obtained above. Electromagnetic analyses of two filters with every different center frequencies were performed and in order to verify the results, the band-pass filter at 3.5 GHz was produced on FR-4 material and S-parameter results were taken. PCB integrated with microstrip technology was used in the design.

Laser cutting method was used in the production process. The pattern of the filter designed over the CST on the computer is processed into the tool. Both surfaces of the FR4 material are coated with copper, and unwanted copper is scraped off with a laser. After the scraping process is completed, the inlet and outlet connectors are soldered so that the filter can be fed. The post-production filter is as shown in Figure 3.12- Figure 3.13.

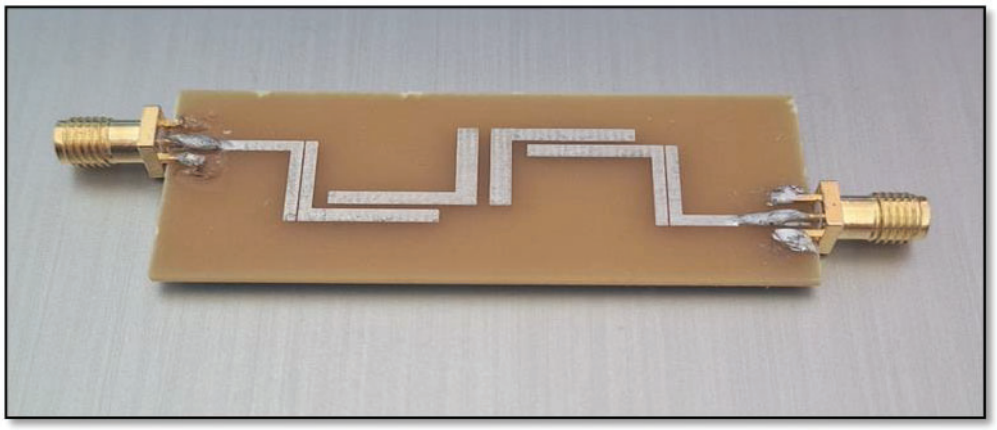


Figure 3.12. Front side of the produced filter



Figure 3.13. Back side of the produced filter

Figure 3.14 shows the S-parameter measurements of the 3.5 GHz bandpass filter together with the Vector Analyzer device. Measurements were carried out with MS4640B serial device of Anritsu. Before the measurement, the transmissions on the line and the impedance value of the filter were checked by means of a multimeter. Since measurements were made at other frequencies before, it was calibrated with an automatic calibration kit.

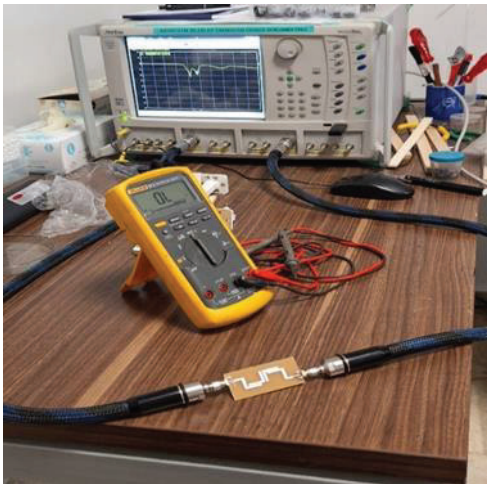


Figure 3.14. Measurement phase of the produced filter

From the measurements, it was observed that the S11 parameter was at -20 dB at 3.49 GHz and values close to the simulation results were obtained.

Figure 3.15 shows the response of the generated filter. A result of -22 dB was obtained for the S_{11} parameter at filter 3.49 GHz. It has been observed from S21 values that the center frequency is at 3.6 GHz, the lower and upper cut-off frequencies are at 3.2 GHz and 3.75 GHz.

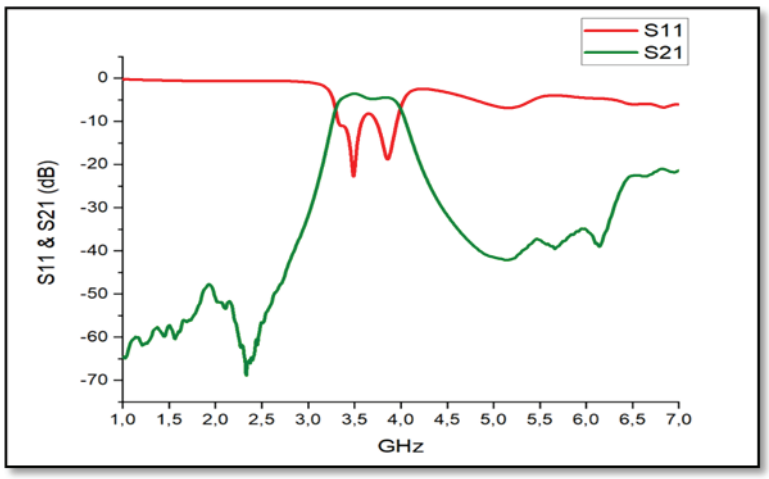


Figure 3.15. Results of the produced filter s_{11} and s_{21}

A comparison of the S11 results of the produced filter and the filter designed in the CST program is made in Figure 3.16. According to the simulation results, a wider band gap was formed. In both results, it is seen that the filter gives the same result for the S11 parameter .

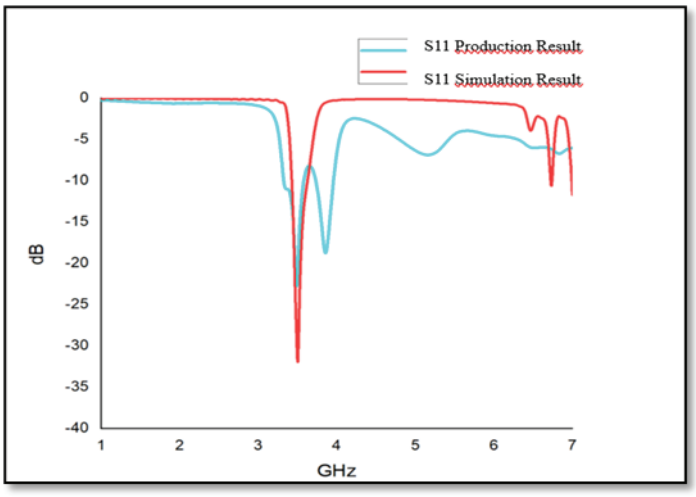


Figure 3.16. S11 Simulation and production result comparison

The S_{21} values of the filter appear to be similar in both results (Figure 3. 17). It is seen that there is a depature from the value close to 0 in the response of the produced filter. The reason for this is thought to be due to filter soldering. It has been observed that unwanted frequencies are suppressed to a good degree.

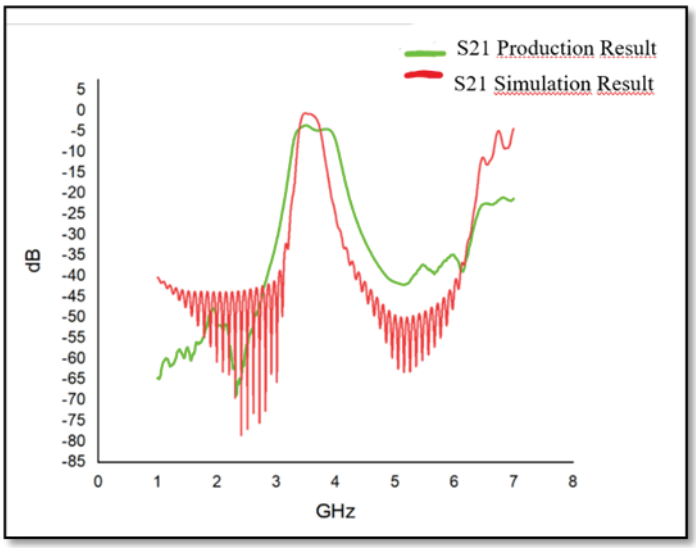


Figure 3.17. S21 Simulation and production result comparison

4. CONCLUSIONS AND RECOMMENDATIONS

In this thesis, a bandpass filter with a center frequency of 3.5 GHz were designed and the results were analyzed.

While our first designed filter was a 4th and 6th degree Butterworth type filter, another design of ours is a filter consisting of interdigital and step impedance parts with imperfect ground. The frequency of the filter are used in the band range called n77, which are used in 5G applications. While the cut-off frequency of Butterworth type filters is 3.5 GHz, While designing the filters, capacitive and inductive values were found by using bulk element calculations. The calculated values were converted into dispersed elements and their drawings were carried out in the CST program. In the program, FR4 material with a dielectric constant of 4.3 was selected for the first designs, while its thickness was taken as 0.8 mm. Copper heights for microstrip transmission lines are defined as 0.035 mm.

In the frequency responses of the Butterworth microstrip filter, fluctuations in the transition regions of the signal are small. Suppression rates down to -80 dB have been observed in the band stop zones. The simulation and measurement results of the filter operating at 3.5 GHz were compared. According to the simulation result, while the S_{11} value is -32 dB in the center frequency, this value is -23 dB as a result of the measurement, similarly, while the S21 values are -0.73 dB as a result of the simulation, it is seen that it is -3 dB as a result of the measurement. In general, the suppression level is below -40 dB. Good immersion rates were obtained in the simulation and measurement results. Looking at the S21 parameter results, it is seen that -0.5 dB levels were obtained in the 300 MHz band range for the first design. the group delays of the filters were at the required levels.

REFERENCES

1. Marconi, G. (1922). Radio telegraphy. *Journal of the American Institute of Electrical Engineers*, 41(8), 561-570.

2. Attaran, M. (2023). The impact of 5G on the evolution of intelligent automation and industry digitization. *Journal of ambient intelligence and humanized computing*, 14(5), 5977-5993.

3. Dahiya, M. (2017). Need and advantages of 5G wireless communication systems. *International Journal*, 5(6).

4. Internet : WHAT IS 5G? URL: https://www.aselsan.com/tr/blog/detay/332/5g-nedir, Last Access Date : 13.04.2024

5. Jia S., Lanchester M. (2001). *Microstrip Filters for RF/Microwave Applications*. John New York: Wiley.

6. Pozar, D.M. (2012). *Microwave engineering,* (3rd edition). New York: Wiley.

7. Afzali, B., Abbasi, H., Shama, F., Dehdasht-Heydari, R. (2021). A microstrip bandpass filter with deep rejection and low insertion loss for application at 2.4 GHz useful wireless frequency. *AEU-International Journal of Electronics and Communications*, 138, 153811.

8. Wang, Z., Fu, Z., Li, C., Fang, S. J., and Liu, H. (2020). A compact negative-group-delay microstrip bandpass filter. *Progress In Electromagnetics Research Letters*, 90, 45-51.

9. Chen, C. F., Li, J. J., Zhou, K. W., Chen, R. Y., Wang, Z. C., and He, Y. H. (2020). Design of a microstrip quad-band bandpass filter with controllable bandwidth and band spacing for multifunctional applications. *IET Microwaves, Antennas & Propagation*, 14(5), 374-380.

10. Balanis, C. A. (2015). *Antenna theory: analysis and design*. New Jersey: Hobokon. 78-120.

11. Geiger R. L. and E. Sánchez-Sinencio, Active filter design using operational transconductance amplifiers a tutorial, *in IEEE Circuits and Devices Magazine,* 2, 20-32, March 1985.

12. Mabrouk, M., and Bousbia, L. (2011). Study and enhanced design of RF dual band bandpass filter validation and confirmation of experimental measurements. *Simulation*, 8(12), 56-61

13. Alexander, C. K., Sadiku, M. (2000). *Electric circuits*. New York: Wiley. 135-150.

14. Zhu, L., Sun, S., and Li, R. (2011). *Microwave bandpass filters for wideband communications*. New York: Wiley. 356-380.

15. Hammerstard, E. O. (1975). *Equations for microstrip circuit design*, in Proceedings of the Eu ropean Microwave Conference, Hamburg, Germany, 268–272.

16. Wheeler, H. (1965). Transmission line properties of parallel strips separated by a dielectric sheet, IEEE Trans., MTT-13, 172–185.

17. Richards, P. I. (1948) *Resistor-Transmission Line Circuits*, Proceedings of the IRE, 217–220.

18. Saleh, S., Ismail, W., Abidin, I. S. Z., Jamaluddin, and M. H. (2020). 5G Hairpin and İnterdigital bandpass filters. *International Journal of Integrated Engineering*, 12(6),71-79.

19. Mahata, S., Herencsar, N., Kubanek, D. (2021). Optimal approximation of fractional-order Butterworth filter based on weighted sum of classical Butterworth filters. *IEEE Access*, *9*, 8107-8114.

20. Sangam, R. S., Dash, S., & Kshetrimayum, R. S. (2020). Ultra-broadband bandpass filter using linearly tapered coupled-microstrip line and open loop defected ground structure. *IEEE Transactions on Circuits and Systems II: Express Briefs*, 68(1), 181-185.

21. Qayyum, A., Khan, A. H., Uddin, S., Ahmad, O., Khan, J. S., and Bashir, S. (2020, November). *A novel mmwave defected ground structure based microstrip antenna for 5G cellular applications*. In 2020 First International Conference of Smart Systems and Emerging Technologies (SMARTTECH*)* IEEE.

22. Lim, J. S., Kim, C. S., Ahn, D., Jeong, Y. C., and Nam, S. (2005). Design of low-pass filters using defected ground structure. *IEEE Transactions on Microwave Theory and Techniques*, 53(8), 2539-2545.

23. Gruszczynski, S., Staszek, K., and Wincza, K. (2023). Parallel-coupled bandpass filters with directly coupled input and output resonators. *AEU-International Journal of Electronics and Communications*, 172, 154974.

24. Darwis, F., Rahayu, E. A. B., Sutrisno, S., Madiawati, H., Taufiqqurrachman, T., Setiawan, A., Wijayanto, Y. N. (2022). Cross-coupled line bandpass filter based on modified parallel-coupled line structure. *Jurnal Elektronika dan Telekomunikasi*, *22*(1), 8-13.

25. Jamsai, M., Angkawisittpan, N., Nuan-On, A. (2021). Design of a Compact Ultra-Wideband Bandpass Filter Using Inductively Compensated Parallel-Coupled Lines. *Electronics*, 10(21), 2575.

26. Sani, A. H., Jianwen, C., Khan, M. T., Yussif, S. B., Nahar, S., Ewald, K. E., Ukwuoma, C. (2019, December). *Design and Simulation of 3.9 GHz Microstrip Parallel Coupled Line Band Pass Filter.* In 2019 16th International Computer Conference on Wavelet Active Media Technology and Information Processing, (429-433).

27. La, D. S., Guan, X., Wang, M. Y., Mi, R. Q. (2021). Compact wideband bandpass filter based on coupled line stub with high selectivity. *AEU-International Journal of Electronics and Communications*, 138, 153872.



Gazili olmak ayrıcalıktır